THE ROLE OF CASPASE-8 IN OLIGODENDROCYTE DEVELOPMENT AND MECHANISMS OF OXIDATIVE INJURY IN NEURONS AND GLIA

A Thesis

by

JEFFREY PAUL THOMPSON

Submitted to the Office of Graduate Studies of
Texas A&M University
in partial fulfillment of the requirements for the degree of

MASTER OF SCIENCE

Approved by:

Chair of Committee,	Jianrong Li
Committee Members,	Jane Welsh
	Louise Abbott
	Paul Wellman
Head of Department,	Evelyn Castiglioni

December 2012

Major Subject: Biomedical Sciences

ABSTRACT

Apoptosis is essential not only to the normal development of a multicellular organism but also for the maintenance of tissue homeostasis. This proposal seeks to investigate, in part, the role of oligodendrocyte (OL) apoptosis in myelination. We used an OL-specific conditional knockout animal to study caspase-8 function in OL development; analyzing histological differences in myelination at postnatal day 10 and alterations to OL proliferation, differentiation, and cell death in culture. Our preliminary data suggests that deletion of caspase-8 did not alter OL proliferation or differentiation in culture, but reduced the percentage of apoptotic cells following nutrient deprivation. *In vivo*, we found an increase in myelinated axons in the spinal cord of caspase-8 deficient mice, indicating a role for caspase-8 in the myelination process.

This study also seeks to investigate mechanisms of cell death in OLs, astrocytes, and neurons following oxidative injury. Exposure of primary OLs, astrocytes, and neurons to arachidonic acid (AA) resulted in oxidative stress and cell death. Necrostation-1, the specific inhibitor of receptor interacting protein kinase 1 (RIP-1), markedly prevented AA-induced oxidative death in OLs and astrocytes, but not in neurons. Similarly, we found that blockade of 12-lipoxygenase (LOX) and c-Jun N-terminal kinase (JNK) protected OLs and astrocytes but not neurons against AA toxicity. Consistent with the inability of necrostatin-1 to rescue neurons, we found very low expression of RIP-1 as well as RIP-3 in neurons. Finally, the zinc chelator TPEN effectively abolished AA-induced oxidative death in all three cell types, suggesting zinc

release as a common mechanism. Taken together, our findings indicate differences in cell death mechanisms following oxidative injury in astrocytes, OLs, and neurons.

ACKNOWLEDGEMENTS

I would like to thank my committee chair, Dr. Jianrong Li, and my committee members Dr. Jane Welsh, Dr. Louise Abbott, and Dr. Paul Wellman for their guidance and support through the course of my studies and in this research.

I would also like to thank my friends, colleagues, and department staff for enriching my experience at Texas A&M. I would also like to thank my family for their love and support throughout my college experience.

NOMENCLATURE

AA	Arachidonic Acid
bFGF	Basic Fibroblast Growth Factor
cDNA	Complimentary DNA
cKO	Conditional Knockout
CNS	Central Nervous System
GFAP	Glial Fibrillary Acidic Protein
JNK	c-Jun N-terminal Kinase
KO	Knockout
LDH	Lactate Dehydrogenase
LOX	Lipoxygenase
OL	Oligodendrocyte
OPC	Oligodendrocyte Precursor Cell
PCD	Programmed Cell Death
PDGF	Platelet Derived Growth Factor
Pre-OL	Pre-Oligodendrocyte
Rho 123	Rhodamine 123
RIP-1	Receptor Interacting Protein Kinase 1
RIP-3	Receptor Interacting Protein Kinase 3
ROS	Reactive Oxygen Species
SVZ	Subventricular Zone

TUNEL	Terminal Deoxynucleotidyl Transferase dUTP Nick End Labeling
WT	Wildtype

TABLE OF CONTENTS

Page

LIST OF FIGURES

LIST OF TABLES

CHAPTER I

INTRODUCTION TO APOPTOSIS AND OXIDATIVE INJURY

Apoptosis

Apoptosis is a form of programmed cell death (PCD) that was first described in mammals 40 years ago (Kerr et al., 1972). Changes in morphological features lead researchers to believe the process was programmed, which was subsequently demonstrated in detail in *Caenorhabiditis elegans* (Yuan et al., 1993). It is now well-established that apoptosis is essential to the development and homeostasis of all multicellular organisms (Jacobson et al., 1997). Apoptosis is a highly regulated process that selected cells undergo (Table 1). Dysregulation of apoptosis could be disastrous for an organism, as is the case in many pathological conditions. For instance, overexpression of anti-apoptotic proteins is often seen in cancers, while wide-spreading apoptotic cascades often increase the damage seen in degenerative conditions such as stroke.

Many mammalian apoptogenic and anti-apoptotic genes have been identified (Metzstein et al., 1998). The central mediators of apoptosis are the caspases. They are a family of cysteine proteases that employ a cysteine residue as the catalytic nucleophile. They exist in the cytoplasm as zymogens. Caspase-8 is known to be an upstream member in apoptosis signaling; it dimerizes and undergoes proteolytic cleavage following the activation of the death-receptors, such as TNF and FAS receptors (Zhao et al., 2010).

Table 1 – Comparison of apoptosis, necroptosis, and autophagy

Factors	Apoptosis	Necroptosis	Autophagy
Morphology	Chromatin condensation, nuclear fragmentation, apoptotic bodies	Organelle swelling, plasma membrane rupture	Autophagic vacuoles
Triggers	Death receptors, trophic factor withdrawal, DNA damage, viral infection	Ischemia, neurodegenerative disease, viral infection	Amino acid starvation, protein aggregation
Mediators	Caspases, BH1-3, BCL2 family proteins	RIP-1/3, JNK, LOX, CYLD	Phosphoinositide -3 kinase, mTOR

Apoptosis, is essential to the development of the central nervous system (CNS) (Hidalgo and ffrench-Constant, 2003), but the role of caspase-8 in CNS development remains unknown. To better understand the function of caspase-8 during development, a complete ablation genetic model was established (Varfolomeev et al., 1998), which was found to be embryonically lethal due to brain and heart malformations (Varfolomeev et al., 1998). Later, it was discovered that brain malformation is likely a secondary issue due to a failure to properly develop yolk sac vasculature in the caspase-8 knockout mice (Sakamaki et al., 2002).

OLs are glial cells in the CNS that ensheath axons with myelin, allowing rapid propagation of action potential (Bunge, 1968, Baumann and Pham-Dinh, 2001, Nicolay et al., 2007). Myelinating OLs are highly differentiated cells. OLs mature during development from oligodendrocyte precursor cells (OPCs), gradually continuing to

mature through different stages, which can be immunohistochemically identified by their distinct surface expression of different proteins and/or certain lipids (Pringle et al., 1992) (Figure 1). OLs primarily develop in early postnatal life from OPCs that migrated from the subventricular zone (SVZ) (Vallstedt et al., 2005). Once positioned, they begin to proliferate and then differentiate and eventually mature into myelin-producing mature OLs (Hardy and Reynolds, 1991, Levison and Goldman, 1993).

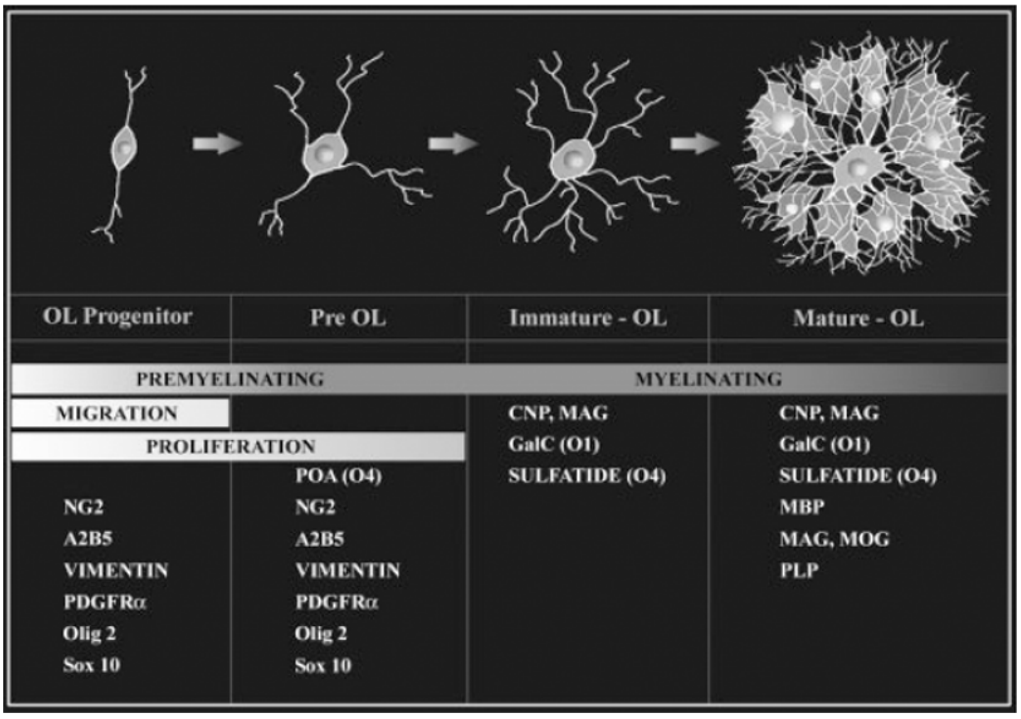

Figure 1 – Oligodendrocyte lineage progression and marker expression. The progression of oligodendrocytes from progenitors to myelinating cells. PDGFR = platelet-derived growth factor receptor; CNP= 2´, 3´-Cyclic nucleotide 3´-phosphodiesterase; MAG = myelin-associated glycoprotein; MBP = myelin basic protein; MOG = myelin oligodendrocyte glycoprotein; PLP = proteolipid protein. Image adapted from Back, S. A. and S. A. Rivkees (2004). "Emerging concepts in periventricular white matter injury." Seminars in Perinatology 28(6): 405-414.

Myelination is a multistep and complex process of which the detailed molecular mechanisms remain incompletely understood. It has been shown previously that OLs receive survival signals from the axons they myelinate (Barres and Raff, 1999). OL lineage cells are produced abundantly during CNS development, and it has been postulated that a competition for survival signals produced by axons leads to appropriate elimination of excess OL lineage cells. Excess OL lineage cells appear to undergo apoptosis (Barres et al., 1992). This process ensures that OLs are matched perfectly to the axonal surface area for subsequent myelination and promotion of action potential propagation (Barres and Raff, 1999). We hypothesized that caspase-8 could be involved in this process of eliminating excess OLs, a possibility that has not been examined previously and was explored in this study.

Although the death-receptors and caspases have been implicated in many neurological disorders, to date, no study has *directly investigated the in-vivo function of caspase-8 in the CNS* during normal development. This is, in part, due to a lack of available conditional caspase-8 knockout mice where caspase-8 is specifically deleted in CNS cells, as global deletion of caspase-8 is embryonically lethal (Busso et al., 2010). To determine the role of caspase-8 in OLs during development, we utilized lox-P Cre technology to specifically ablate caspase-8 in OL lineage cells in mice.

Our study aims to investigate the function of caspase-8 in this context. Since OLs have the potential to myelinate up to 50 axons per cell, alterations in the number of OLs in the developing brain could have a powerful impact on normal brain function. Our

central hypothesis is that *caspase-8 is involved in controlled elimination of superfluous or non-functioning OL lineage cells during development*.

Oxidative injury

Oxidative stress is defined primarily as the loss of a cell's ability to manage the production and elimination of oxidative radicals (Finkel and Holbrook, 2000). Oxidative radicals can be produced by the redox reactions that cells perform on a regular basis for the synthesis and degradation of essential molecules and during energy production in the electron transport chain. It is within the ability of a healthy cell to quickly eliminate radicals produced by normal biological processes with minimal damage. The accumulation of oxidative radicals, such as peroxides and superoxide radicals, can lead to damage. Oxidative stress is involved in many neurological diseases, including stroke (van Leyen et al., 2006), periventricular leukomalacia (Inder et al., 2002), Parkinson's disease (Thompson et al., 2000), and Alzheimer's disease (Behl et al., 1992, Behl et al., 1994).

Oxidative stress is a complex process that can be exacerbated by both intracellular and extracellular stress and/or processes, such as heavy metal release. Zinc has been implicated in oxidative stress (Zhang et al., 2007). It is an abundant trace element in mammals (Weiss et al., 2000, Moos et al., 2007) and the release of intracellular stores, which can be caused by oxidative stress, has been shown to lead to rapid cell death (Choi and Koh, 1998, Frederickson et al., 2005).

AA levels have been shown to increase after brain ischemia (Katsuki and Okuda, 1995). AA is a 20 carbon, omega-6 polyunsaturated fatty acid that can be found in

organs throughout the body and quite abundantly in the brain. It is often a component of the phospholipid bilayer and can be released when phospholipase A2 hydrolyzes the acyl bond of phospholipids, creating free AA. It is involved in cellular signaling as a lipid second messenger. It is also a precursor for the formation of many essential molecules including thromboxane, prostaglandin, prostacyclin, and leukotriene. AA is a known substrate for cycloxygenases and lipoxygenases whose natural metabolism is a source of peroxides and free radicals. Changes in AA metabolism have been implicated in cerebral ischemic injury, inflammation, and several neurological disorders (Simonian and Coyle, 1996, Phillis et al., 2006).

Much of the neurobiological research in the past has focused on the neuron, the functional unit of the brain. In recent years, however, it has become apparent that glial cells are much more than the brain "glue" that their name implies. Astrocytes, in particular, have been found to have numerous functions. Their processes wrap around blood vessels, forming one layer of the blood-brain barrier (Nedergaard et al., 2003). This puts them in a unique position to regulate nutrient trafficking and even carbon dioxide blood levels and blood pH (Gourine et al., 2010). Their processes also contact neuronal synapses and are involved in reuptake of neurotransmitters, including the prevention of excitotoxicity by converting glutamate to glutamine (Liang et al., 2006). They also possess the ability to uptake large amounts of heavy metals such as copper that would be otherwise toxic to neurons (Tiffany-Castiglioni et al., 2011). Due to their many critical functions in maintaining a microenvironment in which neurons can thrive, studying potentially protective mechanisms in pathological conditions is important.

Unfortunately this is often overlooked. In this study we sought to examine the mechanisms occurring in astrocytes following AA-induced oxidative injury, as very little was previously known and astrocytes have the potential to sustain neurons in a toxic environment.

In cell culture, we have previously shown that AA-induced cell death of pre-oligodendrocytes (pre-OLs) is characterized by production of reactive oxygen species (ROS), mediated by 12-LOX activation in the absence of caspase activation (Kim et al., 2010). According to classical morphological indicators such as cellular swelling and membrane rupture, AA clearly induces oxidative stress, leading ultimately to necrosis. We and others have shown that AA-induced cell death is necroptotic, a programmed form of necrosis, as it can be blocked using the RIP-1 inhibitor necrostatin-1 (Degterev et al., 2008, Kim et al., 2010).

Necroptosis is a unique form of programmed cell death. Although it is characterized by morphological hallmarks of typical necrotic cell death such as cellular swelling and membrane rupture, it operates in a programmed, caspase-independent manner (Table 1). Necroptosis is dependent on assembly and activation of RIP-1 and RIP-3 kinases. The RIP kinase family has emerged as critical regulator of cellular fate. RIP-1, in particular, has been shown to be a bifurcation point in cell death signaling, possessing the ability to promote survival or cell death (Vandenabeele et al., 2010). Necrostatin-1 was discovered through chemical library screening and found to be a specific allosteric inhibitor of RIP-1 kinase, which has been shown to be protective in animal models of CNS ischemia (Degterev et al., 2005, Chavez-Valdez et al., 2012) as well as brain

trauma (You et al., 2008), myocardial infarction (Oerlemans et al., 2012), renal ischemia (Linkermann et al., 2012), and systemic inflammatory response syndrome (Duprez et al., 2011). However, it is not clear whether the *in-vivo* protective effects of necrostatin-1 are due to its action on neurons or glia. We therefore investigated the protective potential of necrostatin-1 using the AA-induced oxidative damage model in primary OLs, astrocytes, and neurons. Our central hypothesis was that *necrostatin-1 acts primarily on glial cells to prevent necroptosis following oxidative injury*.

CHAPTER II

METHODS AND MATERIALS

Materials and animals

Dulbecco's Modified Eagle Medium (DMEM), Hank's Balanced Salt Solution (HBSS), Earl's Balanced Salt Solution (EBSS), and fetal bovine serum were purchased from Hyclone (Logan, UT). Human platelet-derived growth factor (PDGF) and basic fibroblast growth factor (bFGF) were from PeproTech (Rocky Hill, NJ). The compound 2,3,5-trimethyl-6-(12-hydroxy-5,10-dodecadynyl)-1,4-benzoquinone (AA861) was purchased from BioMol Research Laboratory (Plymouth, PA). SP600125 was purchased from EMD Chemicals (Gibbstown, NJ). RIP-1 and RIP-3 antibodies were from R&D Systems (Minneapolis, MN) and IMGENEX (San Diego, CA), respectively. Unless specified otherwise, all other reagents were from Sigma (St. Louis, MO). All animal care protocols were in accordance with NIH guidelines for care and use of laboratory animals and were approved by Texas A&M University Laboratory Animal care and use committee.

Generation of oligodendrocyte-specific caspase-8 knockout mice

Conditional knockout mice for caspase-8 were made by utilizing the lox-P Cre system. Mice expressing Cre recombinase behind the OL lineage-specific promotor *Olig 1* (*Olig1*-Cre) were crossed to mice (*Caspase-8*$^{fl/fl}$) expressing lox-P sites within the caspase-8 gene. This resulted in genetic ablation of caspase-8 in OL lineage cells.

Genotyping and PCR

Tail clips of 3 wk old mice were taken and the tissue was digested using a buffer containing 50mM Tris, 20mM NaCl, 1mM EDTA, 1% SDS, and 0.5mg/ml protease k. Samples were heated to 55 °C for 30 min. 500 µl of water was added to each sample and placed in a boiling water bath for 5 min. Samples were then centrifuged for 10 min. at 13.4 rcf and placed on ice immediately. DNA was quantified using a Nanodrop 1000 spectrophotometer (Thermo Scientific). PCR was then performed to test for the presence or absence of *Olig1*-Cre and *Caspase-8*$^{fl/fl}$ using specific primers (Table 2). To check for *Olig1*-Cre we had an initial denaturing step for 3 min at 95°C, then 20 ng of DNA was amplified by 39 cycles of PCR (94°C for 45 sec, 58°C for 1 min, 72°C for 1 min) followed by a final elongation step at 72°C for 3 min. To check for *Caspase-8*$^{fl/fl}$ we had an initial denaturing step for 4 min at 94°C, then 20 ng of DNA was amplified by 30 cycles of PCR (94°C for 30 sec, 62°C for 30 sec, 72°C for 30 sec) followed by a final elongation step at 72°C for 5 min. Samples were electrophoresed in 1% agarose gels and visualized under UV light using a Chemidox XRS gel documentation system (Bio-rad, Hercules, CA).

Table 2 – Genotyping primer sequences (conditional knockout mice)

Gene Name	Forward Sequence (5′ - 3′)	Reverse Sequence (5′ - 3′)
Olig1-Cre Wildtype	GTGTTCCAAGGAGCGA TGTAGTTGCTTGGG	CTCCTAGATCCGCATG GTTTGGCTGGAGAG
Olig1-Cre Mutant	GGACATGTTCAGGGAT CGCCAGGCG	GCATAACCAGTGAAAC AGCATTGCTG
Caspase-8$^{fl/fl}$	ATAATTCCCCCAAATC CTCGCATC	TCCTGTACCATATCTGC CTGAACGCT

Primary glial cell cultures

Primary glial cultures were prepared from the forebrains of 1- to 2-day old Sprague-Dawley rat pups using a differential detachment method as previously described (McCarthy and de Vellis, 1980). Once the meninges were removed from the forebrains, the tissue was briefly digested using HBSS containing 0.1% trypsin and 10 μg/ml DNAse. The cells were then triturated in DMEM containing 10% heat-inactivated fetal bovine serum and 1% penicillin-streptomycin. Dissociated cells were plated onto 75 cm^2 poly d-lysine coated flasks and the medium was changed every other day for 7 days.

Isolation of oligodendrocytes

After shaking of the cells for 1 hour to remove microglia, the cultures were shaken overnight at 200 rpm to isolate pre-OLs. This cell suspension was then plated onto uncoated petri dishes to further remove contaminating microglia/astrocytes. The resulting pre-OLs were plated onto poly-ornithine coated plates and maintained in a serum-free defined medium (BDM, 0.1% bovine serum albumin, 50 μg/ml human apo-

transferrin, 50 μg/ml insulin, 30nM sodium selenite, 10nM d-biotin, and 10 nM hydrocortisone in DMEM) supplemented with 10 ng/ml PDGF and 10 ng/ml bFGF for 7-9 days at 37°C in a humid atmosphere of 5% CO_2 and air. Culture medium was half changed every other day, and the cells were used experimentally between 7-9 days *in-vitro* (DIV).

Isolation of astrocytes

After the isolation of OLs, cell cultures were washed once with phosphate buffered saline (PBS). Briefly, the cultures were treated with DMEM medium containing 0.1% trypsin at 37°C. Cells were suspended in DMEM medium containing 10% fetal bovine serum and centrifuged at 9.3 rcf for 7 minutes. Medium containing trypsin was aspirated and cells were suspended in previously mentioned media. Cells were plated on 75 cm^2 poly d-lysine coated flasks and allowed to grow to confluency. The cells were then treated with 1 μM L-leucine methylester for 1 hr at 37°C to eliminate contaminating microglia. Cells were washed once with PBS and trypsinized as previously mentioned. Astrocytes were then plated on poly d-lysine coated plates and maintained in the described medium for 1-3 days before experimental use.

Primary neuron cultures

Cultures were taken from the forebrains of embryonic (E) day 16.5 Sprague-Dawley rat pups. Briefly, forebrains free of meninges were dissected in cold dissection buffer (Ca^{2+}/Mg^{2+}-free HBSS containing 10mM HEPES), and then dissociated with papain (10 units/ml) in dissection buffer for 5 min at 37°C. Cells were then treated with trypsin inhibitor (10 mg/ml) in dissection medium for 2-3 min. After 2 additional washes with

trypsin inhibitor solution, the cells were suspended in plating medium (Neurobasal, 2% B27, 1 mM glutamine, 25 μM glutamic acid, 100 units/ml of penicillin, and 100 μg/ml streptomycin). The cells were then passed through a 70 μm cell sieve and live cells were counted using a hemocytometer and trypan blue exclusion assay. Mature cortical neuron cultures were cultured for 14-20 days and purified by adding 10 μM fluorodeoxyuridine (FdU) and 10μM uridine diluted in neurobasal medium. FdU treatment began on DIV 1, and cells were cycled through 2 days of treatment and 2 days without treatment for a total of 3 FdU cycles. Immature neurons were cultured for 3-7 days and purified by adding 5 μM arabinofuranosyl cytidine (ara-c) diluted in neurobasal media for 48-72 hrs.

Immunohistochemistry

Cell cultures were fixed with 4% paraformaldehyde immediately following viability analysis. Cells were then washed 3 times in tris-buffered saline (TBS) for 5 min, following by a 1 hr blocking and permeabilizing step using 5% goat serum and 0.1% Triton-X diluted in TBS. Primary antibodies were incubated overnight, diluted in TBS as indicated below. All secondary antibodies were purchased from Invitrogen and diluted to a concentration of 1:1000 in blocking solution, then incubated 1 hr at room temperature.

Transmission electron microscopy

Mice were anesthetized and perfused using PBS and then fixed with 20 ml PBS containing 2% paraformaldehyde and 2.5% glutaraldehyde (Electron Microscopy Sciences, Halflield PA) then post-fixed overnight at 4°C. The brains, spinal cords, and optic nerves were collected. The brains were then segmented using a mouse-specific

alto 0.5 mm stainless steel matrix (Roboz Surgical Instrument Company, Inc. Gaithersburg, MD) and trimmed to 2-3 mm thick segments. Spinal cords were cut into 3-5 mm segments coronally. The tissues were then washed in 0.1M sodium cacodylate buffer and stained using 1% osmium tetroxide and 0.5% potassium ferrocyanide in 0.5% sucrose for 1.5 h. Next, the tissues were serially dehydrated in ascending alcohol series and embedded in epoxy resin. Ultrathin sections of the tissue were examined with an FEI Morgagni 268 transmission electron microscope at an accelerating voltage of 80 kV. Digital images were acquired with a MegaViewIII camera operated with iTEM software (Olympus Soft Imaging Systems, Germany). Image contrast was uniformly adjusted with Adobe Photoshop. The number of myelinated axons was determined from 4400x fields from each region and was expressed as axons per mm^2.

Reverse transcription PCR

RNA was isolated 5 hrs after AA treatment as described using the RNEasy Kit (Qiagen, Valencia, CA). Samples were reverse transcribed into cDNA using a reverse transcription kit (Promega, Madison, WI) and random primers in the presence or absence of reverse transcriptase for 10 min at 25°C, followed by 15 min at 45°C, 5 min at 95°C, and 5 min at 4°C. PCR was then performed to test for the presence or absence of RIP-1 and RIP-3 using specific primers (Table 3). Primers for GFAP and Iba-1 were used to examine glial contamination in neuron cultures (Table 3). The housekeeping gene actin was used as a control (Table 3). To check for RIP-1 we had an initial denaturing step for 10 min at 95°C, then 100 ng of cDNA was amplified by 30 cycles of PCR (95°C for 15 sec, 56°C for 15 sec, 72°C for 30 sec) followed by a final elongation step at 72°C for

5 min. To check for RIP-3 the initial denaturing step was for 2 min at 94°C, then 100 ng of cDNA was amplified by 35 cycles of PCR (94°C for 30 sec, 60°C for 30 sec, 72°C for 1 min) followed by a final elongation step at 72°C for 10 min. To check for GFAP we had an initial denaturing step for 5 min at 95°C, then 100 ng of cDNA was amplified by 30 cycles of PCR (95°C for 5 sec, 62°C for 30 sec, 72°C for 1 min) followed by a final elongation step at 72°C for 7 min. To check for Iba-1 and Actin we used an initial denaturing step for 5 min at 95°C, then 100 ng of cDNA was amplified by 30 cycles of PCR (95°C for 45 sec, 57°C for 45 sec, 72°C for 45 sec) followed by a final elongation step at 72°C for 5 min. Samples were electrophoresed in 1% agarose gels and visualized under UV light using a Chemidox XRS gel documentation system (Bio-Rad, Hercules, CA).

Table 3 – RTPCR primer sequences (rat)

Gene name	Forward sequence (5′ - 3′)	Reverse sequence (5′ - 3′)
RIP-1	GCACCAGCTGTCAGGGCCAG	GCCCAGCTTTCGGGCACAGT
RIP-3	GCACCAGCTGTCAGGGCCAG	GCCCAGCTTTCGGGCACAGT
GFAP	AGGAAGGGTACTGCCTCCCCC	CCACACACAGCCTCCCTCAGC
Iba-1	CTTTTGGACTGCTGAAAGCC	GTTTCTCCAGCATTCGCTTC
Actin [a]	GCATGCAGAAGGAGATCACA	ACATCTGCTGGAAGGTGGAC

a – primer sequence is for mouse actin

Western blots

Cell lysates were subjected to SDS-polyacrylamide gel electrophoresis followed by electrotransferring onto PVDF membranes. Nonspecific binding was blocked by incubating the membrane in TBS-T (50nM Tris-HCl, pH 7.4, 150mM NaCl, 0.1% Tween-20) containing 5% skim milk for 1 hr at room temperature. Anti RIP-1 (1:1000 dilution, Mse IgG, R&D Systems, MAB 3585), RIP-3 (1:1000 dilution, Rabbit IgG, Imgenex, IMG-5523-1), and β-actin (1:10,000 dilution, Sigma, A2066) antibodies were diluted in TBS-T containing 5% skim milk and incubated overnight at 4°C. The membrane was then washed 3-5 times using TBS-T and incubated with horseradish peroxidase conjugated secondary antibody (1:1000) for 1 hr with agitation. After 4-5 washes with TBS-T, protein bands were visualized by chemilluminescence using the SuperSignal detection kit (Thermo Scientific, Rockford, IL).

Arachidonic acid treatment

To induce oxidative stress, freshly prepared AA (stock concentration 100 mM in anhydrous dimethyl sulfoxide [DMSO]) was added to cells in BDM medium. The co-treatment drugs necrostatin-1, baicalein, vitamin K_2, and SP600125 were also made in anhydrous DMSO and diluted from 20mM, 100mM, 10mM, and 50mM stock solutions, respectively. TPEN and AA861 were made in ethanol and diluted from 100mM and 10mM stock solutions, respectively. All drugs were added at the same time as AA. The final concentration of DMSO in the culture medium was $\leq 0.1\%$ and had no effect on cell viability, proliferation, or morphology. DMSO was used as a vehicle control in all experiments.

Viability assays

Cell viability was determined 16-20 hrs after treatment using Alamar Blue (Southern Biotechnology, Birmingham, AL), a tetrazolium dye that is reduced by living cells to a colored product. All results of cell death assays were confirmed by visual inspection of cells under a phase contrast light microscope. Survival assays were performed in triplicate, and the results were expressed as mean ± SEM. In some cases, cell toxicity was assessed by lactate dehydrogenase (LDH) release assay (Roche Diagnostics, Indianapolis, IN). Briefly, culture medium was collected at the end of experiments and analyzed for LDH release according to the manufacturer's protocol.

Intracellular reactive oxygen species detection

Intracellular free radical accumulation was visualized using dihydrorhodamine 123 (Rho 123; Invitrogen, Carlsbad, CA) as previously described (Kim et al., 2010). Rho 123 was made in DMSO and diluted from a 10mM stock. Cells were treated for 4-6 hrs with AA, and then 10μM Rho 123 diluted in culture medium was added to the cells for 20 min. at 37°C. The extracellular dye was then removed by washing the cells with warm EBSS twice. Live cell imaging using Rho 123 was visualized under a fluorescent microscope (Olympus IX71) equipped with an Olympus DP70 digital camera. Microscope settings such as brightness, contrast, and exposure time were held constant to compare intensities of oxidized Rho123 across conditions.

Live cell staining

Astrocytes were treated with AA for 3 hrs and then either 1 μM FluoroZin-3 (Invitrogen), 20nM Mitotracker Red (Invitrogen), or 1 μg/ml JC-1 (Invitrogen) was

added and incubated for 20 min. at 37ºC. In addition, we incubated 50 nM DND-99 (Invitrogen) for 5 min at 37ºC. The cells were then washed twice with warm EBSS and viewed live under a fluorescent microscope (Olympus IX71) equipped with an Olympus DP70 digital camera. Microscope settings such as brightness, contrast, and exposure time were held constant to compare intensities across conditions.

Statistical analysis

All cell culture experimental conditions were performed in triplicate. GraphPad Prism software was used for data analysis. One-way ANOVA with a Bonferroni Posthoc test was used to determine statistical significance unless otherwise indicated. $P<0.05$ was considered statistically significant. Results are presented as mean ± SEM. $P<0.05$, *; $P<0.01$, **; $P<0.001$, ***.

CHAPTER III

RESULTS

Apoptosis

Generation of oligodendrocyte-specific caspase-8 knockout animals

OL lineage–specific caspase-8 conditional knockout (cKO) mice were generated by mating mice that have exon 2 of the caspase-8 gene floxed to mice expressing cre recombinase behind the OL-specific promotor *Olig1*. Expression of cre recombinase resulted in excision of the floxed exon 2, rendering the gene nonfunctional (Figure 2A). To verify the deletion of caspase-8 specifically in OLs, we designed primers that bind to the introns upstream and downstream of the lox-P sites (Figure 2A). When exon 2 is deleted, the primers amplify a 200 base pair band (Figure 2B). The absence of a 700 base pair wild type (WT) band confirms the animal is a cKO (Figure 2B). Because *Olig1*-Cre is a knockin mutant, homozygous expression of the *Olig1*-Cre allele causes a nonfunctional Olig1 gene, resulting in a lethal phenotype around 2 weeks of birth (Xin et al., 2005). Therefore, animals heterozygous for *Olig1*-Cre and homozygous for *Caspase-8*$^{fl/fl}$ were used as conditional caspase-8 KO mice for this study.

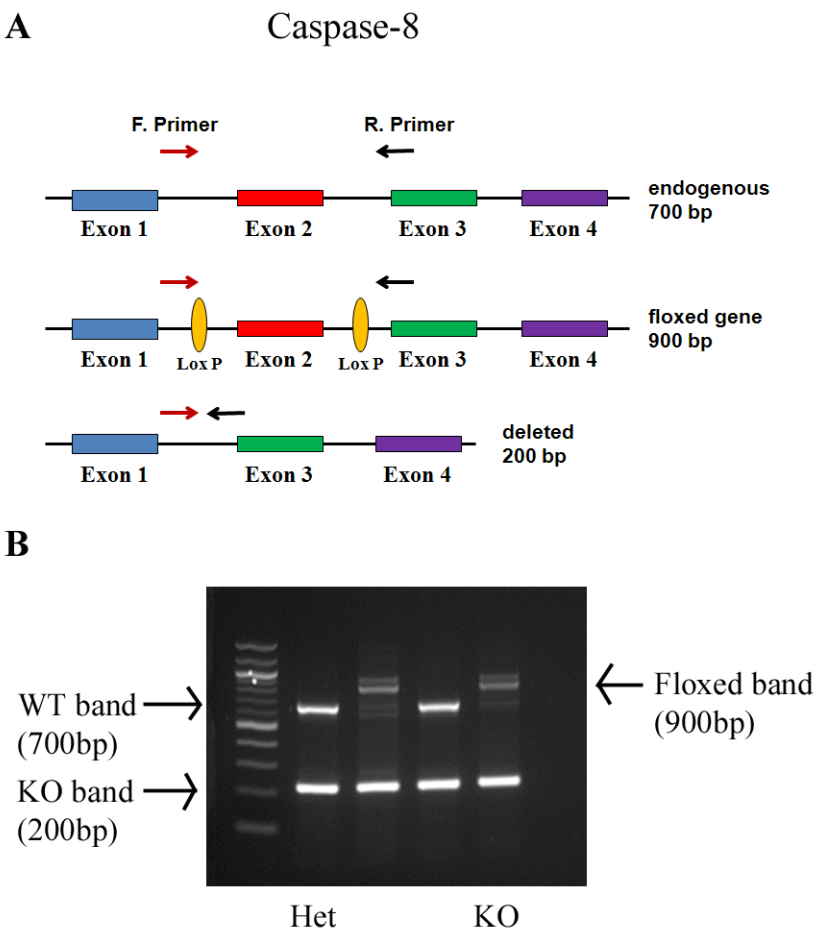

Figure 2 – Caspase-8 deletion strategy. (A) Specific primers were designed to bind outside of exon 2. When exon 2 is deleted, a 200 bp band is produced. (B) PCR results with primers from panel A. Heterozygous animals contain one KO and one WT band. KO animals contain one KO band and partial expression of a floxed band. Het = heterozygous, KO = knockout.

Conditional knockout of caspase-8 in oligodendrocyte lineage cells leads to an increased number of oligodendrocytes in culture

To determine the effect of caspase-8 ablation in OLs, mixed glial cultures from cKO and heterozygous mice were cultured in different media. Cells were cultured in either DMEM medium containing 1% fetal bovine serum (D1S), BDM (0.1% bovine serum albumin, 50 µg/ml human apo-transferrin, 50 µg/ml insulin, 30nM sodium

selenite, 10nM d-biotin, and 10 nM hydrocortisone in DMEM), or minimal DMEM media for 3 days, and were analyzed by immunocytochemistry for changes in total cell number, proliferation, and differentiation. The OL transcription factor Olig2 was used to identify OL lineage cells in the culture grown in D1S medium. Comparing the number of $Olig2^+$ cells across genotypes revealed that there were significantly more OLs in cKO cultures compared to heterozygous littermate controls ($P < 0.001$, Figure 3A).

Caspase-8 deletion in oligodendrocyte lineage cells does not change oligodendrocyte precursor cell proliferation in culture

To determine why there were more OLs present in cKO cultures, we first analyzed OPC proliferation. The OPC marker A2B5 and the OL markers Olig2, and O4 were used to identify the OL lineage cells in the mixed glial culture. Analysis of the percentage of proliferating OPCs grown in D1S medium, as determined by Ki67 and Olig2 double positive OLs divided by the total number of $Olig2^+$ OLs, revealed that ablation of caspase-8 in OLs did not affect the cell proliferation ($P > 0.05$, Figure 3B).

Deletion of caspase-8 does not affect the differentiation of oligodendrocytes in culture

We next investigated possible changes in OPC differentiation due to caspase-8 deletion. BDM media is the minimal media that allows for OL growth and differentiation; therefore we analyzed the OLs under this experimental condition to determine if there were any differences in OPC differentiation due to the deletion of caspase-8. Olig2 staining was again used to determine the total number of OL lineage cells while the OL surface marker O4 was used to distinguish more differentiated OLs.

The percentage of differentiated, $O4^+$ OLs was found to be statistically the same across all genotypes ($P > 0.05$, Figure 3C).

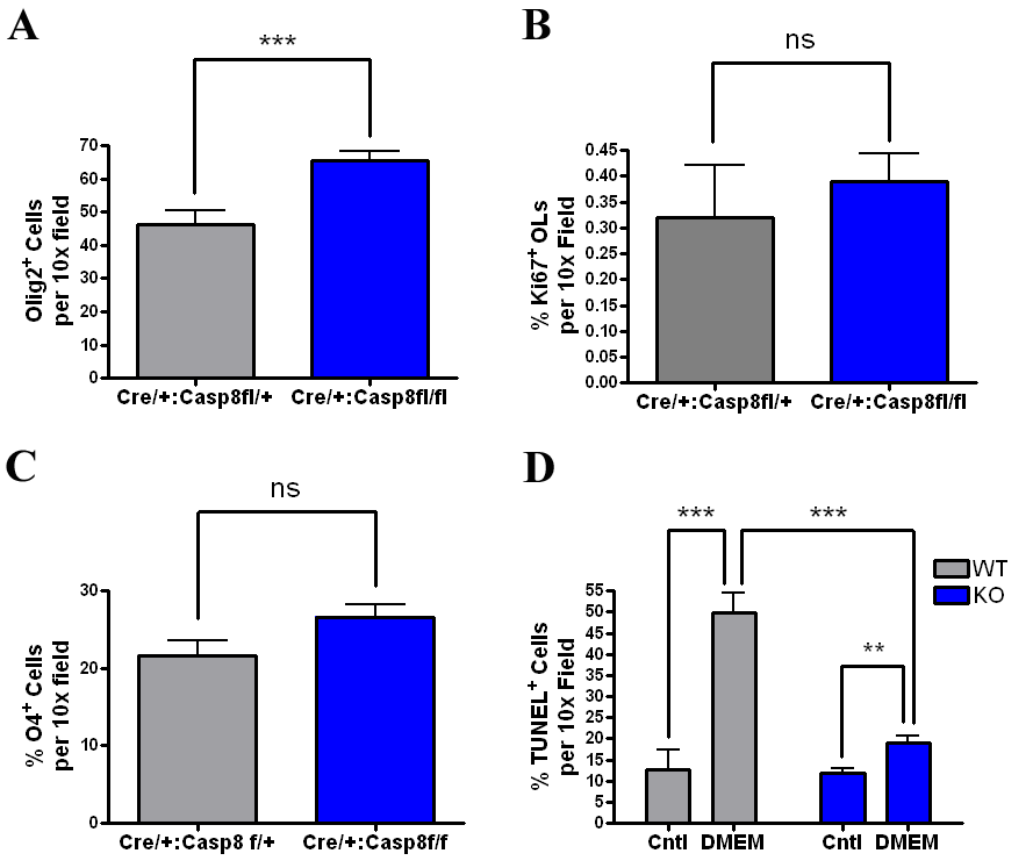

Figure 3 – Effects of caspase-8 deletion in oligodendrocyte physiology in culture. (A) The numbers of total $Olig2^+$ cells were compared across genotypes. (B) The percentage of $Ki67^+$ OLs were calculated by dividing the number of Ki67, Olig2 double positive cells by the total number of $Olig2^+$ cells and compared across genotypes. (C) The percentage of $O4^+$ cells were calculated by dividing the number of O4, Olig2 double positive cells by the total number of Olig2+ cells and compared across genotypes. (D) The percentage of $TUNEL^+$ cells were calculated by dividing the number of TUNEL, DAPI double positive cells by the total number of DAPI positive cells and compared across genotypes. n=1-2 independent experiments. Data analyzed using Student's t-test.

Deletion of caspase-8 in oligodendrocyte lineage cells decreases cell death following nutrient deprivation

OL cell cultures subjected to nutrient deprivation have been shown to undergo apoptosis (Barres et al., 1992). Therefore, we subjected isolated OLs to minimal DMEM media and stained WT and cKO cultures using terminal deoxynucleotidyl transferase dUTP nick end labeling (TUNEL) to identify apoptotic cells. In WT cells, nutrient deprivation caused a significant increase in $TUNEL^+$ cells ($P < 0.001$, Figure 3D). In contrast, in caspase-8 deficient OLs, nutrition deprivation induced apoptotic cell death was significantly less as compared to WT ($P < 0.001$, Figure 3D).

Caspase-8 deletion leads to an increase in myelinated axons in the spinal cord of postnatal day 10 mice

Postnatal day 10 animals were perfused and the brains, spinal cords, and optic nerves isolated for transmission electron microscopy. It was found that brain sections at this time point were minimally myelinated in the corpus callosum (Figure 4C). In the spinal cord, however, there was a significant increase in the number of myelinated axons in cKO animals as compared to littermate WT ($P < 0.01$, Figure 4A, B). Optic nerve samples were visually inspected for robust differences and a modest increase in myelination was noted (Figure 4C). Further quantification was needed to confirm this observation.

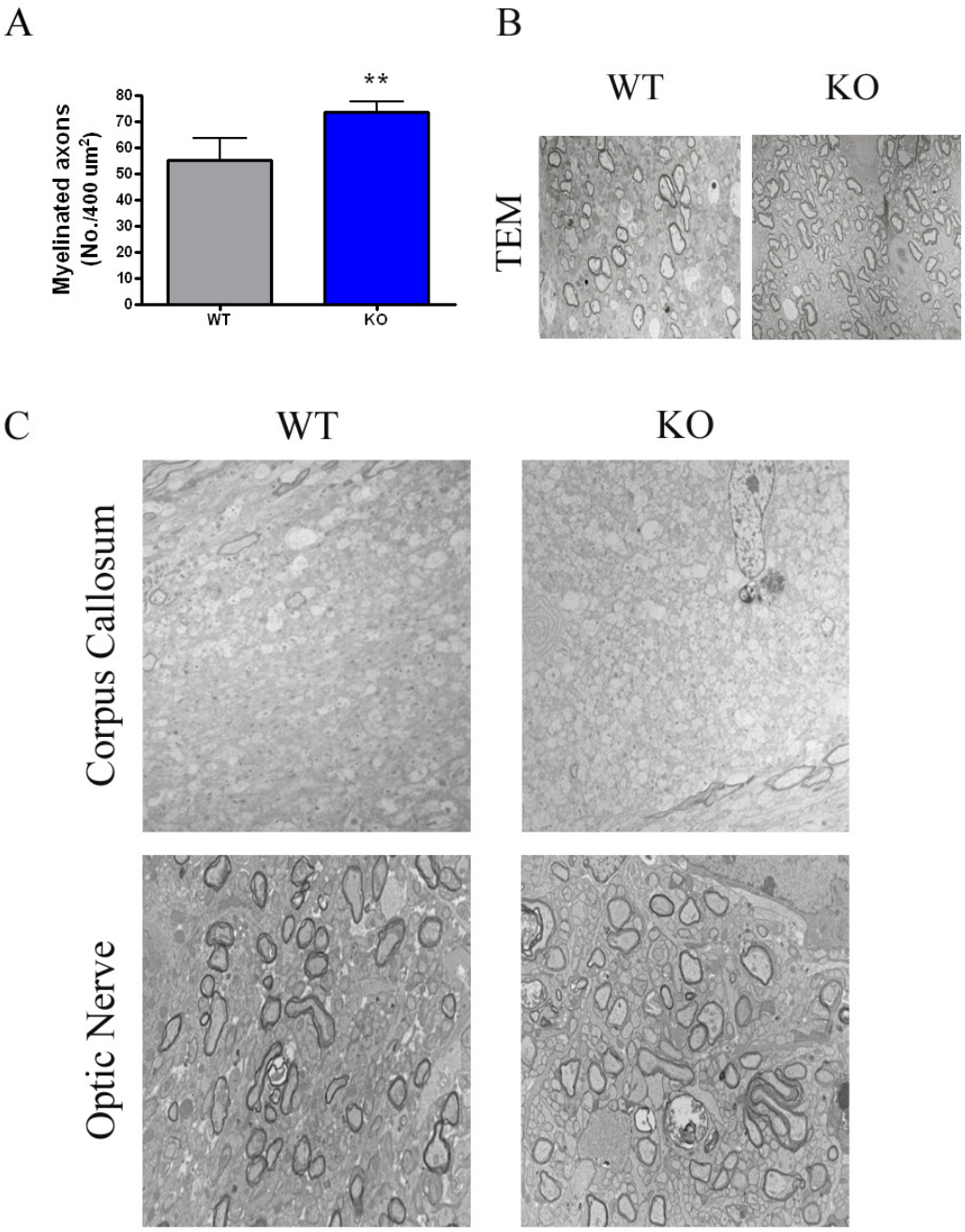

Figure 4 – Caspase-8 deletion in oligodendrocytes results in more myelinated axons in P10 spinal cord. (A) Myelinated axons were counted in 1800x TEM images of coronally sectioned P10 spinal cords. Results yielded a p-value < 0.01. n=3 animals/WT, n=4 animals/KO. (B) Representative TEM microscopy images of the spinal cord taken from animals of different genotypes. (C) Representative images of the corpus callosum and optic nerve from different genotypes. Data analyzed using Student's t-test.

Oxidative injury

Arachidonic acid induces oxidative stress in oligodendrocytes

To determine the effect of AA on OLs, isolated OLs were treated with AA overnight in the presence or absence of 12-LOX inhibitors baicalein (1 μM) and AA861 (10 μM), the JNK inhibitor SP600125 (7.5 μM), or 1 μM vitamin K_2. Exposure of OLs to AA resulted in cellular swelling and reduced cell viability ($P < 0.001$, Fig. 5A,C). Blockade of 12- LOX with AA861 but not baicalein prevented OLs from cell death ($P < 0.001$, $P > 0.05$, respectively, Figure 5A, D, E), indicating the involvement of 12-LOX in AA-induced OL cell death. AA861 appeared to be consistently toxic to neurons; therefore baicalein was used for all of the following neuron experiments. Inhibition of JNK by SP600125 and co-treatment with vitamin K_2 each resulted in a significant protective effect ($P < 0.001$, Figure 5A, F, G). These results are consistent with our previous findings that AA causes 12-LOX activation and subsequent ROS production, leading to cell death (Kim et al., 2010) and that vitamin K_2 is protective to developing OLs by inhibiting 12-LOX (Li et al., 2009).

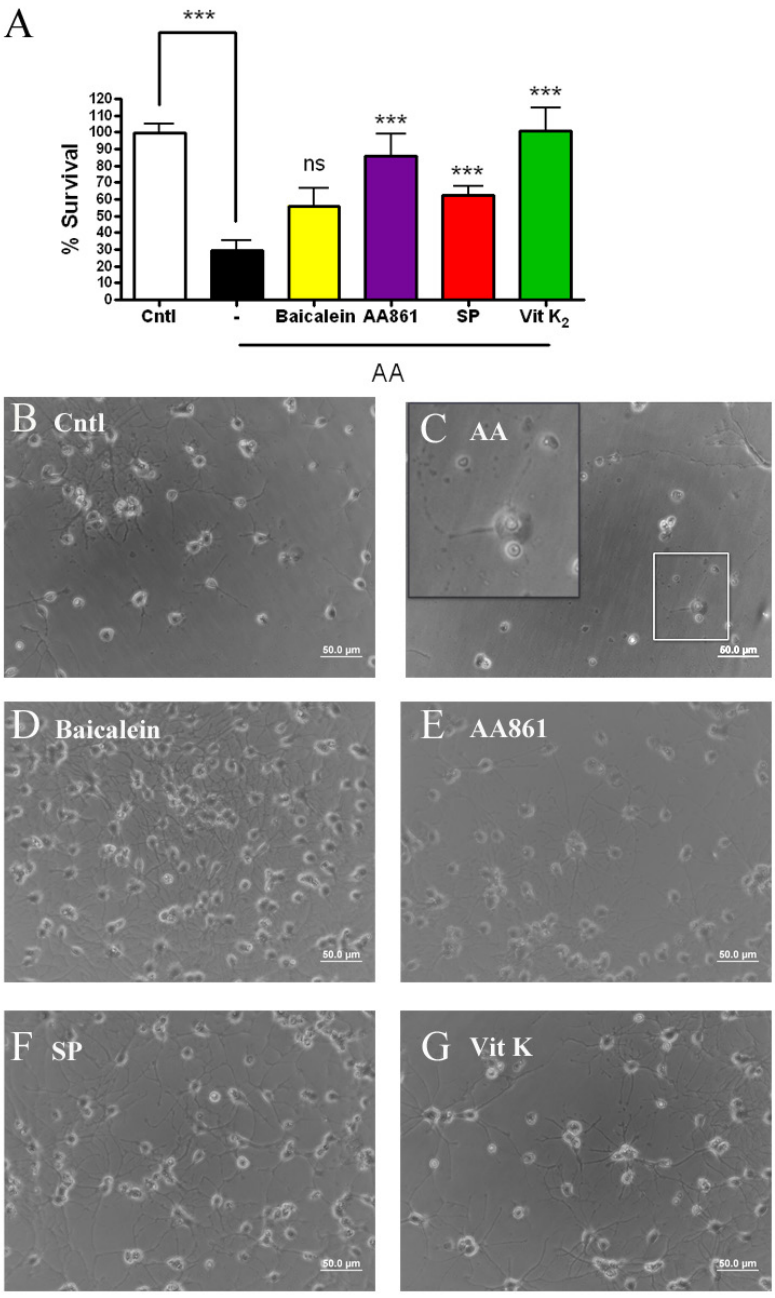

Figure 5 – Arachidonic acid induces oxidative stress in oligodendrocytes. (A) Isolated OLs were treated with 60µM AA in the presence or absence of 2µM baicalein, 10µM AA861, 7.5µM SP600125, or 1µM vitamin K_2. Cell viability was analyzed. (B-G) Representative phase contrast images for control (B), AA treated in the absence (C), or presence of baicalein (D), AA861 (E), SP600125 (F), or vitamin K_2 (G). Scale bar = 50 µm. n=3-6 independent experiments for all drugs tested.

Arachidonic acid induces oxidative stress-mediated cell death in cortical neurons

To examine whether AA also causes cytotoxicity in primary neurons, we treated mature cortical neurons (DIV 14-20) with AA overnight in the presence of 1 μM baicalein, 7.5 μM SP600125, or 1 μM vitamin K_2. AA treatment resulted in similar morphological changes in neurons as in OLs, and neuronal viability decreased significantly ($P < 0.001$, Fig. 6A, C). Co-treatment with either 12-LOX or JNK inhibitors (baicalien and SP600125, respectively) did not attenuate the loss of cell viability ($P > 0.05$, Figure 6A). Vitamin K_2, however, was able to partially prevent cell death ($P < 0.01$, Figure 6A).

Since protein expression can change during the development of the brain and result in differences in susceptibility to certain stressors, these experiments were repeated in immature neurons (DIV 4-7). We found that AA again induced cell death ($P < .001$, Figure 6B) and neither 12-LOX nor JNK inhibitors ameliorated neuronal cell death ($P > .05$, Figure 6B). For both immature and mature neurons, vitamin K_2 was partially protective ($P < 0.01$, Figure 6A, B). To test whether the neuronal cell death was related to oxidative stress, we measured cell viability after co-treatment with the classical anti-oxidant α-tocopherol (1 μM) and found that it was indeed protective in mature neurons ($P<.05$, Figure 6A) and caused a 36.37% increase in viability in immature neurons based on 2 independent experiments.

OLs have been shown to produce large amounts of ROS after AA treatment (Kim et al., 2010). Therefore, we measured ROS production using Rhodamine-123, a compound for live-cell imaging that becomes fluorescent when oxidized by peroxides

and free radicals. Neurons were found to produce ROS after AA treatment although not as robustly as OLs (Figure 6C).

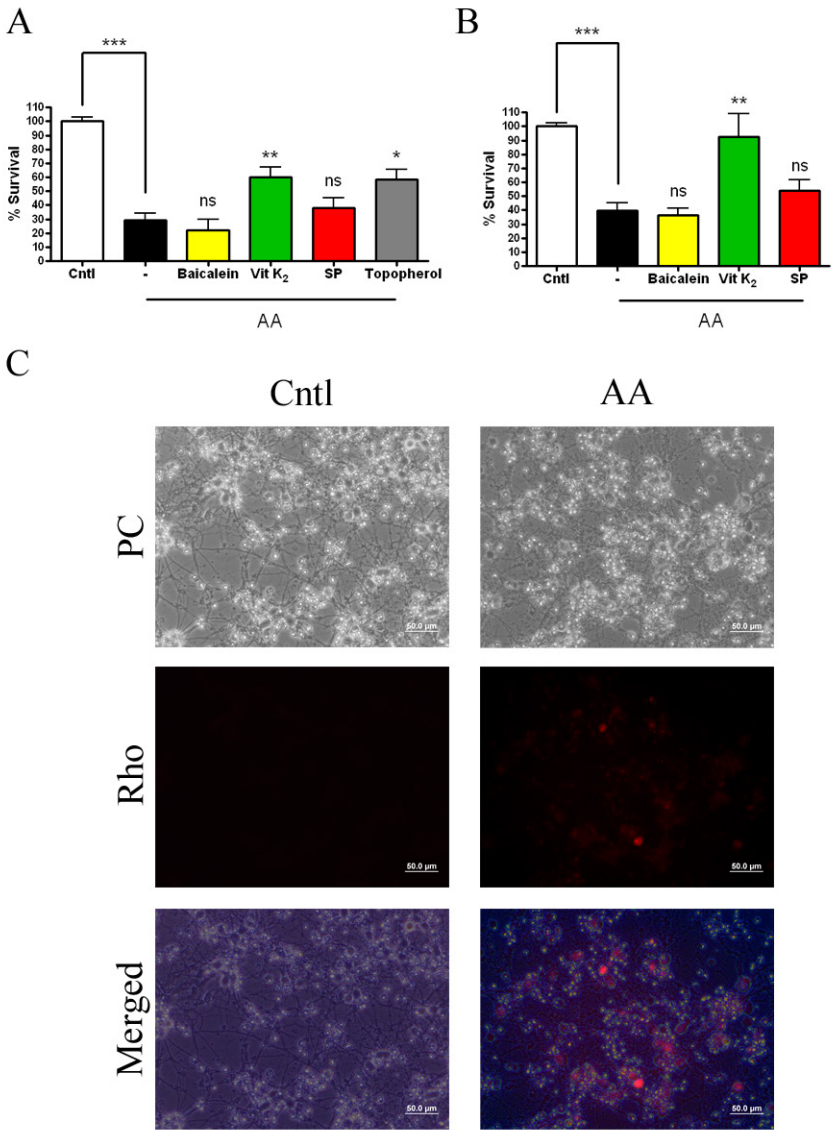

Figure 6 – Arachidonic acid induces oxidative stress in neurons through different mechanisms. (A-B) Mature (A) or immature (B) cortical neurons were treated overnight with AA in the presence or absence of 1μM baicalein, 1μM vitamin K_2, 7.5μM SP600125, or 1μM tocopherol. Cell viability was analyzed. (C) Neurons were treated with AA for 5 hrs and then 10μM Rhodamine 123 was diluted into the medium. ROS production was compared across treatment groups. n=3-6 independent experiments for all drugs tested.

Oxidative injury in astrocytes treated with arachidonic acid

Because neurons and OLs differed in response to AA, we next asked whether astrocytes and OLs share a common cell death pathway. Astrocytes were co-treated overnight with AA and 5 μM baicalein, 7.5 μM SP600125, or 1 μM vitamin K_2. Upon AA treatment, astrocyte viability was decreased ($P < 0.001$, Figure 7A, C). Blockade of 12-LOX with baicalein conferred significant protection ($P < 0.01$, Figure 7A, D). Co-treatment with vitamin K_2 resulted in complete protection against AA-induced cell death ($P < 0.001$, Figure 7A, F). So did the JNK inhibitor SP600125 ($P < 0.01$, Figure 7A, E). Although astrocytes exposed to AA exhibited cell swelling similar to that of OLs and neurons they developed large vacuoles in their cytoplasm (see below) that were not observed in neurons and OLs.

Alternative mechanisms in astrocytes under oxidative stress

Astrocyte responses to AA-induced oxidative injury mirrored that seen in OLs, suggesting a common cell death mechanism among glial cells. There was however a distinct difference in morphology in astrocytes treated with AA; they formed a large number of vacuoles in the cytoplasm (Figure 8B). We reasoned that the vacuoles forming in AA-treatment astrocytes were probably autophagosomes, a hallmark of cells undergoing autophagy (Table 1). We therefore tested the protective potential of autophagosome formation inhibitors 3-methyladenine (3-MA) and bafilomycin A1. Bafilomycin appeared to have a modest protective effect, causing a 9.3% increase in viability (Figure 8C, F) based on 2 independent experiments. 3-MA appeared to be mildly toxic to astrocytes, causing a change in astrocyte morphology and a 15.39%

decrease in viability when co-treated with AA (Figure 8C, E). It remained to be determined whether blocking the formation of autophagosomes confers any protective effect in astrocytes.

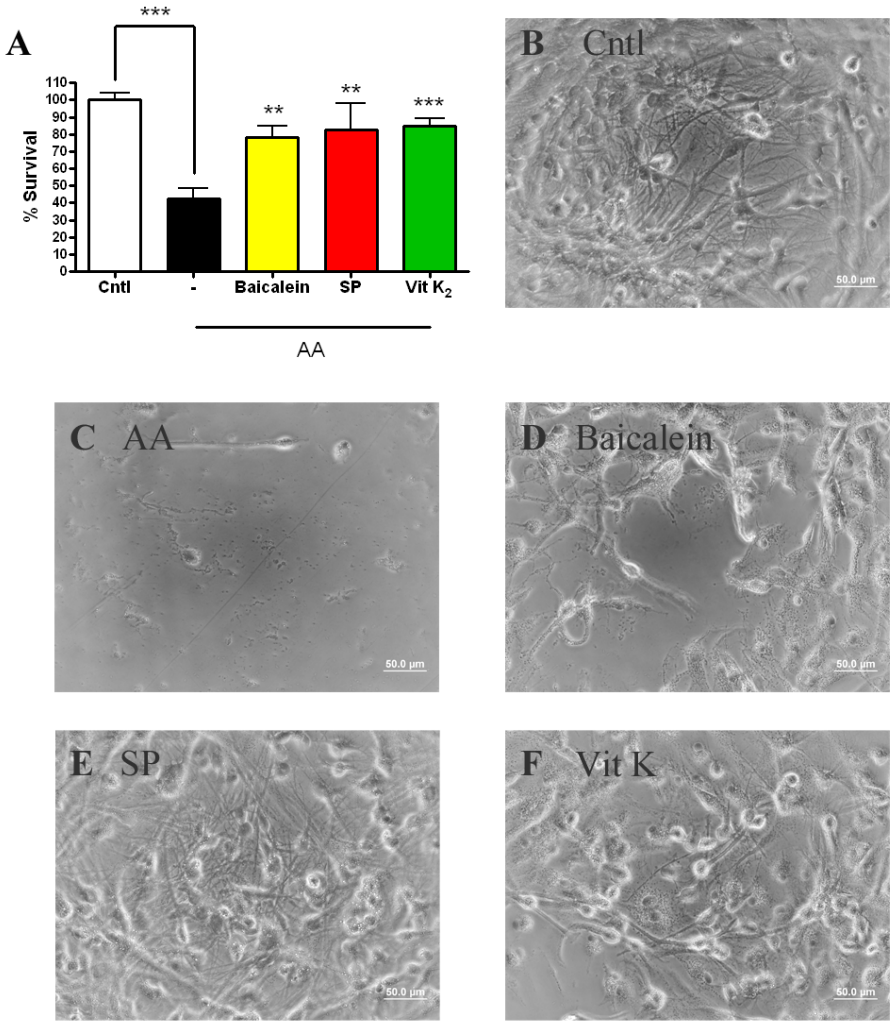

Figure 7 – Arachidonic acid induces oxidative stress in astrocytes. (A) Astrocytes grown 2-3 days in culture were treated with AA in the presence or absence of 5µM baicalien, 7.5µM SP600125, or 1µM vitamin K_2. Cell viability was analyzed. (B-F) Representative phase contrast images of control (B), AA treated in the absence (C), or presence of baicalein (D), SP600125 (E), or vitamin K_2 (F). Scale bar = 50µm. n=3-5 independent experiments for all drugs tested.

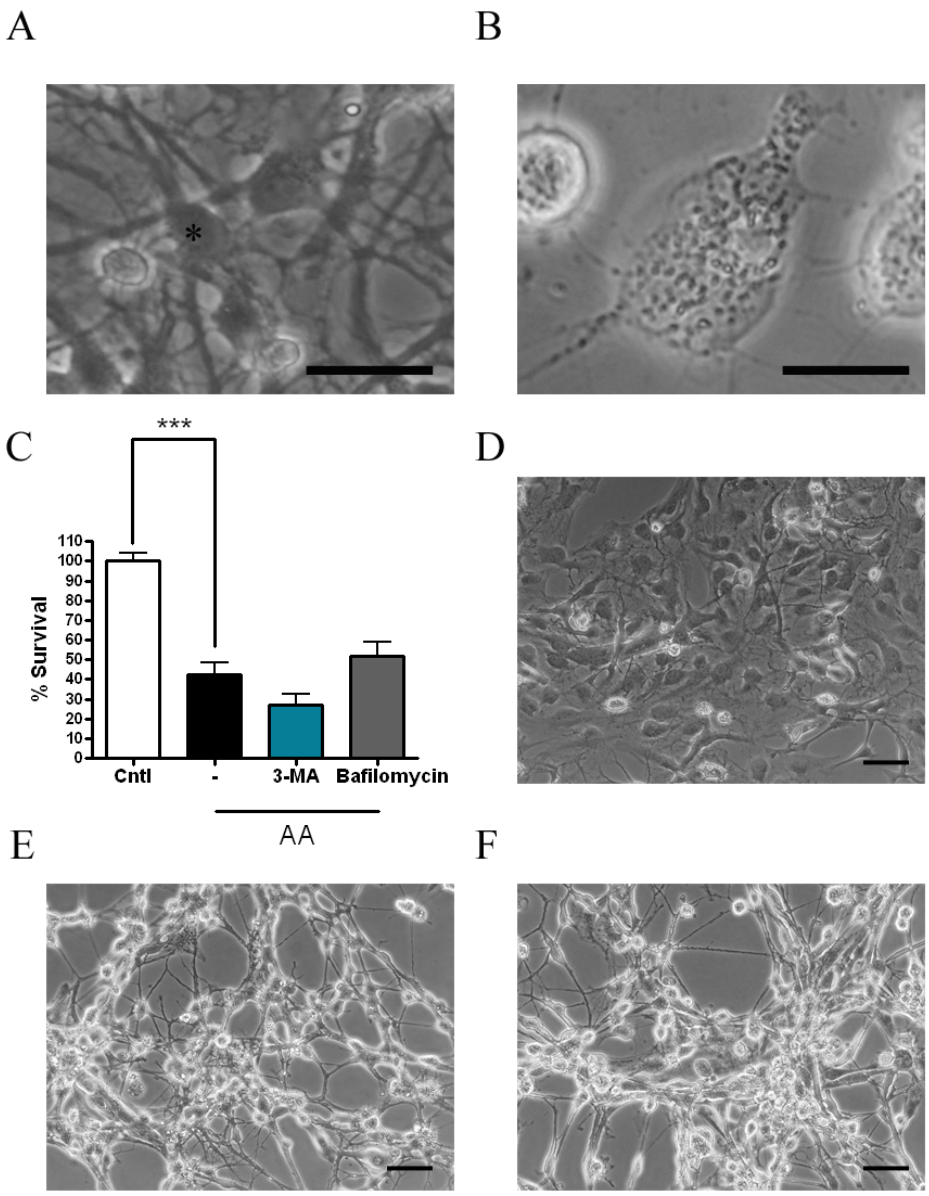

Figure 8 – Alternative mechanisms in astrocytes under oxidative stress. (A-B) Representative phase contrast images from control astrocytes (A,*) and AA-treated astrocytes (B). (C) Astrocytes were treated overnight with AA in the presence or absence of 2mM 3-Ma or 10nM bafilomycin. Cell viability was analyzed. n=2 independent experiments for 3-Ma and bafilomycin, n=6 for control and vehicle conditions. Data analyzed using Student's t-test. (D-F) Representative phase contrast images of control (D), AA in the presence of 3-Ma (E), or bafilomycin (F). Scale bar = 25 μm (A,B), scale bar = 50 μm (D-F).

Live cell imaging in astrocytes

To examine the nature of these vesicles, we used a fluorescent dye to monitor lysozyme formation (300nM LysoTracker). After AA treatment, LysoTracker imaging appeared to show a significant increase in lysosome formation (Figure 9). Additionally, cells were stained with JC-1 (1mg/ml) and mitotracker red (20nM) to evaluate changes in mitochondrial health after AA treatment. We utilized JC-1 as an indicator of alterations in the mitochondrial membrane potential. We did not observe obvious alterations in mitochondrial membrane potential across treatment groups, as the red/green ration appeared very similar (Figure 9). There was a noticeable reduction in mitotracker red staining, which suggests an overall decrease in mitochondrial health (Figure 9).

Zinc release in arachidonic acid-induced oxidative injury

The heavy metal zinc has been linked to both autophagy and oxidative stress (Lee et al., 2009). To examine the possible involvement of zinc in oxidative injury, we co-treated astrocytes with AA and the zinc chelator TPEN (400nM) and AA. TPEN nearly completely abrogated AA-induced cell death ($P < .001$, Fig. 10A). To further verify the involvement of intracellular zinc release, we then used the zinc-specific fluorescent dye FluorZin-3 (1μM) to visualize the location and quantity of zinc in the cell. Following AA treatment, there appeared to be a more diffuse cytoplasmic staining which may be indicative of intracellular zinc release (Figure 10B). TPEN co-treatment was also tested in oligodendrocytes and caused a 65.65% decrease in cytotoxicity based on 2 independent experiments (Figure 10C). In neurons, TPEN co-treatment lead to a

54.03% decrease in cytotoxicity based on 1 experiment (Figure 10D). Cytotoxicity was determined by measuring the levels of lactate dehydrogenase in the culture medium.

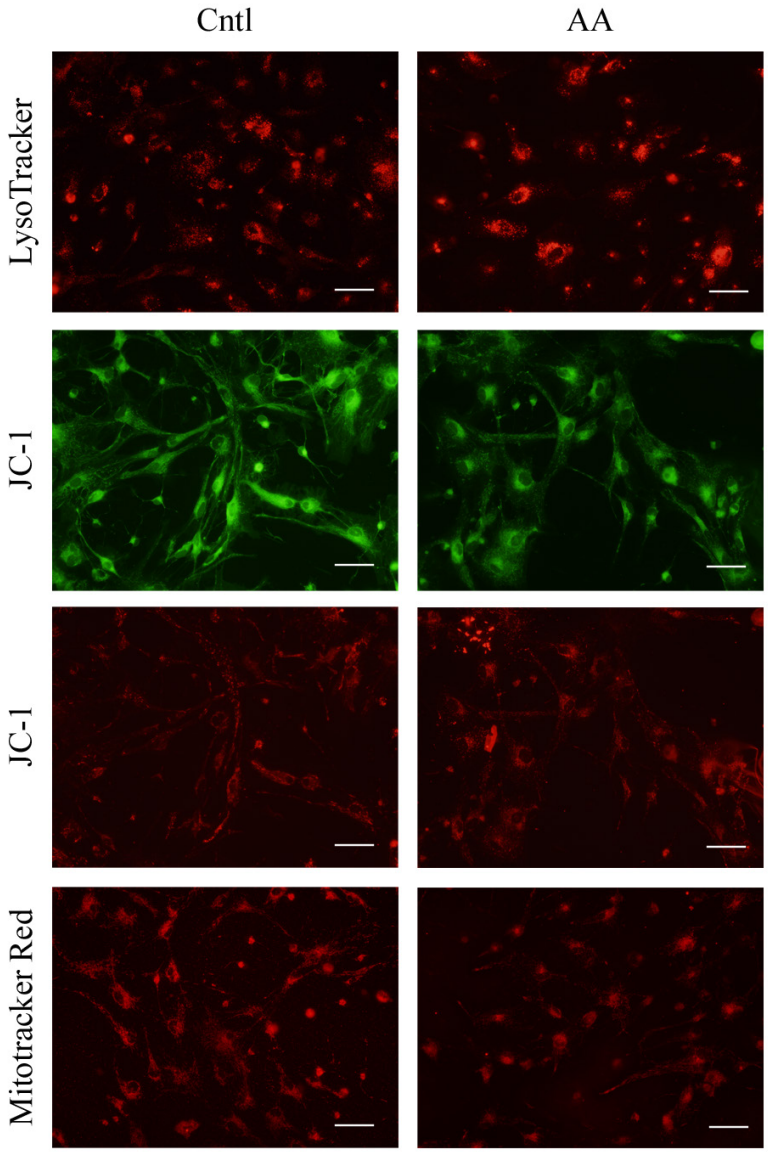

Figure 9 – Live cell imaging of astrocyte lysosome formation and mitochondrial health. Astrocytes were treated with AA for 3 hrs and then either 50nM LysoTracker, 1μg/ml JC-1, or 20nM Mitotracker Red were added to the culture media. Images are representative of control (left column) and AA-treated (right column) experimental conditions. Scale bar = 50 μm.

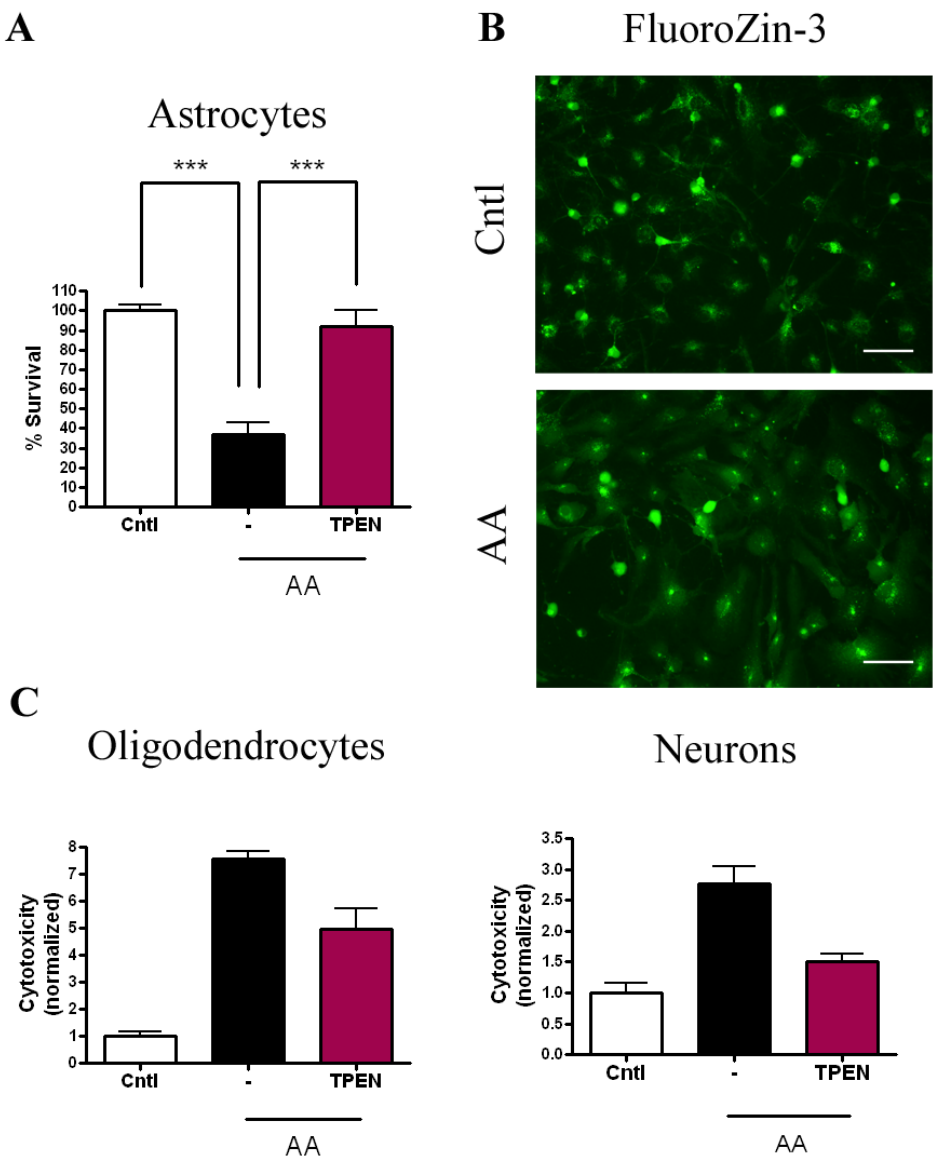

Figure 10 – Zinc release following arachidonic acid treatment. (A) Astrocytes were treated with AA overnight in the presence or absence of 500nM TPEN. Cell viability was analyzed. n=4 independent experiments. (B) Astrocytes were treated with AA for 3 hrs and then 1μM Fluorozin-3 was added to the culture medium. A comparison between treatment groups was made. Scale bar = 50 μm. (C-D) Cultures were treated identically to panel A for OLs (C) and neurons (D) with n=2 and n=1 independent experiments, respectively.

Involvement of receptor interacting protein kinase 1 in arachidonic acid-induced cell death

We have previously demonstrated that RIP-1 becomes activated in OLs after AA treatment and is responsible for their necroptotic cell death, since co-treatment with the allosteric RIP-1 inhibitor necrostatin-1 completely abolished AA toxicity (Kim et al., 2010). We were able to repeat these findings in our paradigm and found that necrostatin-1 treatment was protective in OLs ($P < .001$, Figure 11A). Necrostatin-1 also attenuated AA-induced cell death ($P < .001$, Figure 11B). In contrast, necrostatin-1 had no protective effect against AA-induced toxicity in immature and mature cortical neurons ($P > .05$, Figure 11C, D).

Neurons express low levels of receptor interacting protein kinase 1

To further investigate why necrostatin-1 was ineffective in neurons, we then examined RIP-1 expression in cultured neurons. RNA and proteins from mature and immature neurons treated with AA for 5 hrs were extracted and subjected to RT-PCR and Western blotting analysis respectively. Neurons were found to express mRNA for RIP-1 (Figure 12A). However, RIP-1 protein was expressed at very low levels in neurons as compared to that in glial cells ($P < 0.05$, Figure 12B, C). Since OLs, microglia, and astrocytes all express RIP-1 mRNA, we asked whether RIP-1 mRNA in our neuronal cultures were due to residual glial cell contamination. The purity of the isolated cultures was verified with the exception of microglial contamination in OL cultures and mild astrocyte contamination in mature neuron cultures (Figure 12A).

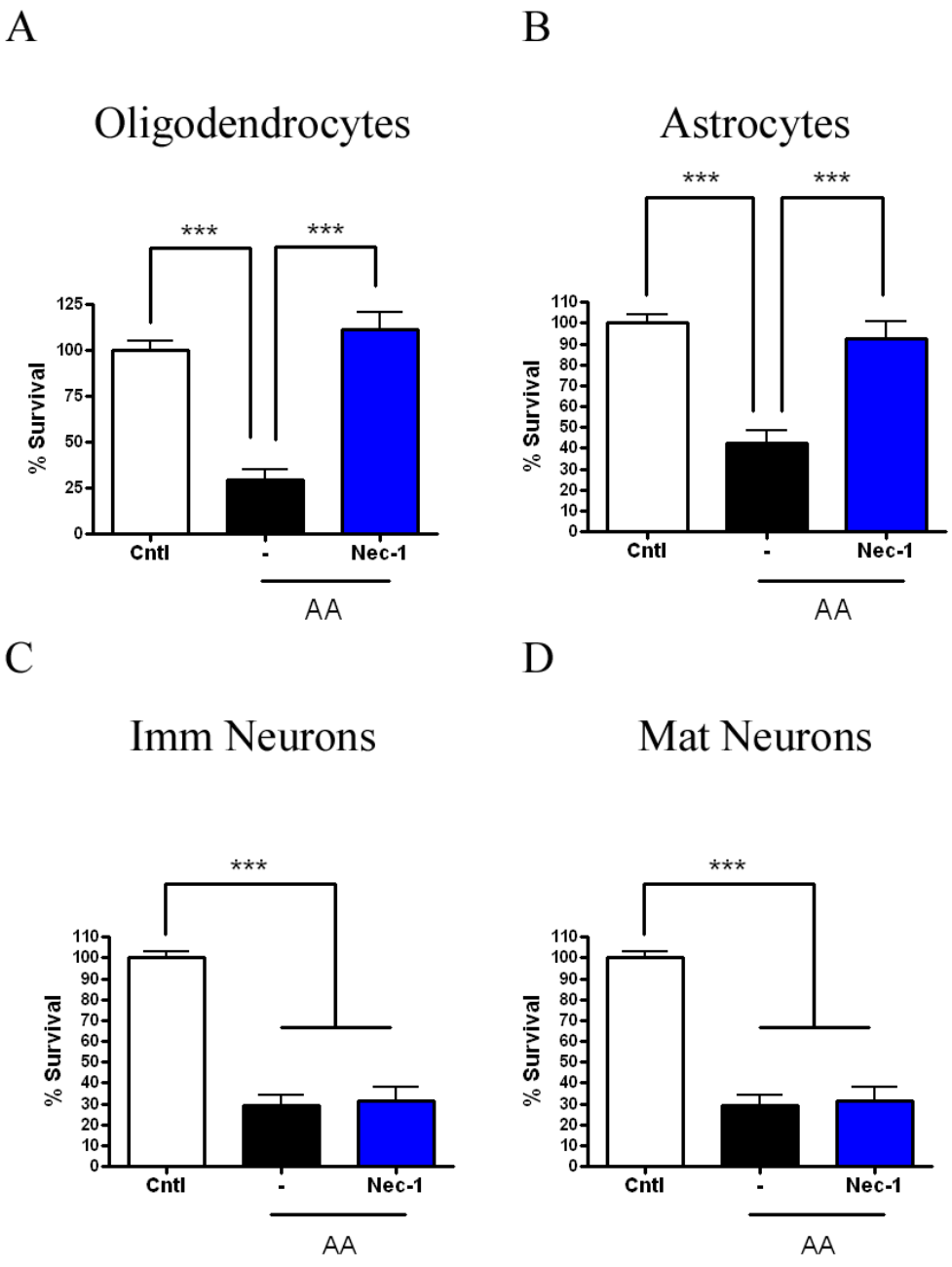

Figure 11 – Receptor interacting protein kinase 1 involvement in arachidonic acid-induced toxicity. (A-D) Cell cultures were treated overnight with AA in the presence or absence of 20μM necrostatin-1. Cell viability was analyzed in OLs (A), astrocytes (B), immature neurons (C), and mature neurons (D). n=3-5 independent experiments.

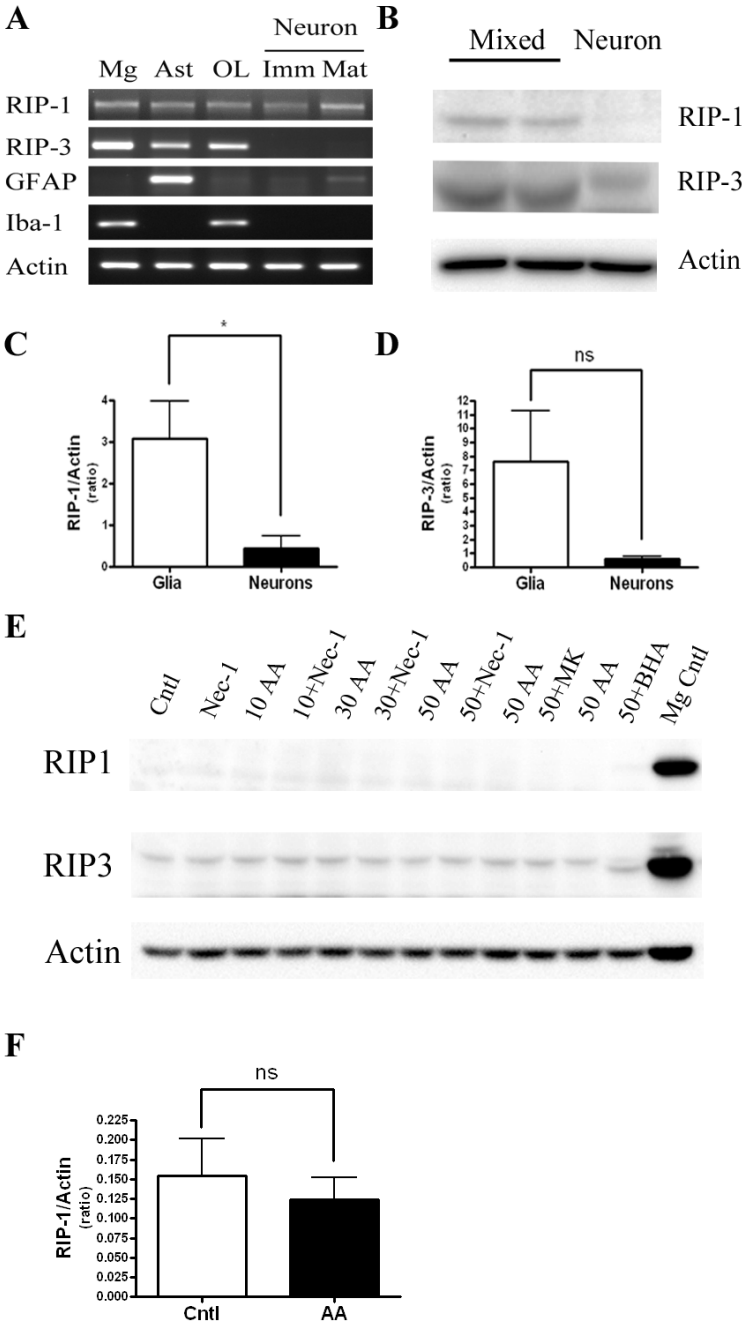

Figure 12 – Receptor interacting protein kinase 1 expression in neurons and glia. (A) RT-PCR using cDNA from unstimulated cells checking for expression of RIP-1, RIP-3, GFAP, Iba-1, and β-actin. (B) A western blot for RIP-1, RIP-3, and β-actin in unstimulated glial and neuronal cultures. (C) Densitometry normalizing RIP-1 (C) and RIP-3 (D) expression levels to β-actin in unstimulated neurons and glia. (E) A western blot for RIP-1, RIP-3, and β-actin in neuronal cultures with or without AA treatment. (F) Densitometry normalizing RIP-1 expression levels to β-actin in stimulated and unstimulated neuronal cultures. MK = MK801, BHA = butylated hydroxyanisole, Mg = microglia. n=3-5 independent experiments. Data analyzed using Student's t-test.

RIP-3 is a cognate kinase to RIP-1 and has been shown be to a crucial member of a multi-protein complex to leads to necroptosis (Vandenabeele et al., 2010). OLs, microglia, and astrocytes were found to express RIP-3. Neurons, interestingly expressed little to no RIP-3 at the mRNA and protein level ($P > .05$, Figure 12A, B, D).

To determine if RIP-1 expression could be increased under oxidative stress, we extracted protein from neurons treated in AA and investigated changes in RIP-1 and RIP-3 expression. We did not observe any increase in expression in cortical neurons under oxidative stress ($P > .05$, Figure 12E, F). Taken together, cortical neurons appear to have minimal expression of RIP-1 and RIP-3, which may account for the inability of necrostatin-1 to protect them from AA-induced oxidative injury.

CHAPTER IV

CONCLUSION

Apoptosis

Apoptosis is a unique form of programmed cell death characterized by morphological hallmarks such as nuclear condensation, membrane blebbing, and cell shrinkage (Raff, 1998). It is known to be essential for the healthy development of the CNS (Yuan and Yankner, 2000). Since OLs are produced in numbers larger than seen in the adult brain, the superfluous cells have to be eliminated (Barres et al., 1992, Barres and Raff, 1994). This is accomplished by apoptosis. A better understanding of cell death mechanisms in OL development could potentially lead to better therapeutics in demyelinating diseases such as multiple sclerosis, periventricular leukomalacia, and other leukodystrophies where decreasing number of OLs has been associated with the pathogenesis (Nave, 2010). Our preliminary data suggests that deletion of caspase-8 in OL lineage cells leads to precocious myelination in the spinal cord and that deletion of caspase-8 does not affect OPC proliferation or differentiation in culture. It does, however, prevent nutrient deprivation-induced apoptosis (Figure 13).

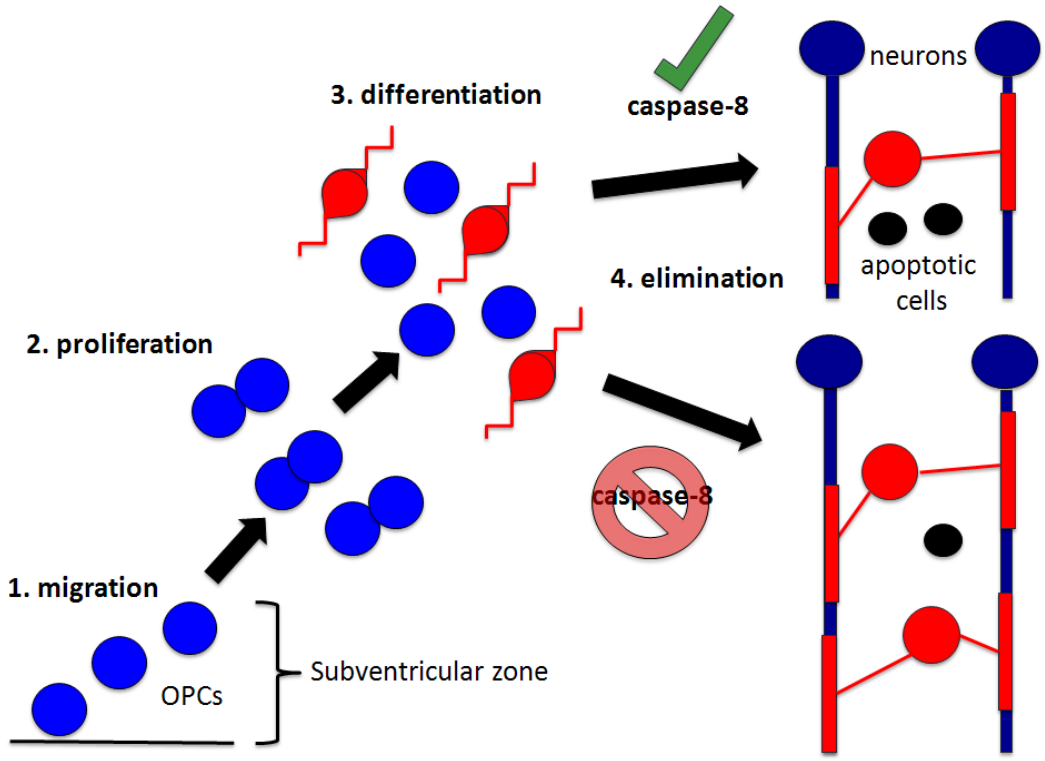

Figure 13 – Proposed schematic of caspase-8 involvement in olligodendrocyte development. Caspase-8 deletion does not have an effect on OPC proliferation or differentiation *in-vitro*. Deletion of caspase-8 did, however, lead to fewer apoptotic cells following nutrient deprivation *in-vitro* and more myelinated axons in P10 spinal cord *in-vivo*.

Recently caspase-8 has been shown to have functions influencing healthy physiology, especially in immune cells (Siegel, 2006, Koenig et al., 2008, Burguillos et al., 2011). Therefore, it was necessary to examine the effect of caspase-8 deficiency on normal OL physiology such as the rate of proliferation and the ability to differentiate. OL proliferation and differentiation, in particular, are critical processes in CNS myelination (Hardy and Reynolds, 1991, Levison and Goldman, 1993). Mixed glial cultures prepared from WT and cKO mice were cultured in D1S media for 3 days, more OLs were found in the caspase-8 cKO cultures (Figure 3A). Further investigation

revealed that the increase in $Olig2^+$ cells in the cKO mixed glial cultures was not due to an increase in the rate of cell proliferation (Figure 3B) nor due to more differentiated OLs (Figure 3C). Instead, the difference was likely due to an inhibition of OL lineage cell death in culture (Figure 3D). Apoptosis can be initiated by multiple stimuli, including nutrient deprivation. Further studies need to be conducted to investigate the effect of caspase-8 deletion as on death receptor, TNF and Fas induced OL apoptosis. Caspase-8 is classically involved in receptor-induced apoptosis, it is worth noting that these were only preliminary experiments, having been performed only once and need to be repeated several times before a definitive conclusion can be made. Nevertheless, our preliminary results were in line with our hypothesis that caspase-8 deletion in OL lineage cells would impair apoptotic cell death.

In-vivo, ablation of capsase-8 leads to an increase in the number of myelinated axons in the spinal cord at postnatal day 10 (Figure 4A, B). At postnatal day 10, there was minimal myelination in the brain to compare across genotypes (Figure 4C). Initial visual inspection of the optic nerve revealed a possible difference across genotypes but the number of myelinated axons needs to be counted before a conclusion can be drawn (Figure 4C). The spinal cord and optic nerve are myelinated very early in development; therefore the difference we noticed across genotypes in the spinal cord could be occurring in the brain as well at a later time point. In the future, proliferation, differentiation, and cell death markers need to be utilized in immunohistochemical analysis of developmental tissues at different time points.

In conclusion, this portion of our study began the investigation into the role of caspase-8 in OL lineage cells during normal CNS development. In addition to the need to repeat the experiments performed in this study, further studies can be conducted to investigate the function of caspase-8 in demyelinating pathological states as well as an impact on remyelination. Apoptosis of OLs is thought to be involved in numerous pathological conditions, such as prenatal white matter injury due to hypoxia/ischemia (Hu et al., 2000, Lesuisse and Martin, 2002, Feng et al., 2003). Additionally, dysregulation of programmed cell death has been implicated in neurodegenerative, traumatic, ischemic, metabolic, and demyelinating disorders (Nakamura and Lipton, 2009, Kuo et al., 2010, Qin et al., 2010, Gregory and Pound, 2011). Direct use of antibodies against cleaved caspases as therapeutics has also been demonstrated to reduce neurodegeneration (Friedlander et al., 1997, Yang et al., 1998, Ona et al., 1999, Galvan et al., 2006). Therefore, the advancement of understanding in the role of programmed cell death in CNS pathology could lead to viable cellular targets to reduce or prevent damage in a tissue that has little to no self-regenerative capacity.

Oxidative injury

Oxidative stress is defined primarily as the loss of a cell's ability to manage the production and elimination of oxidative radicals (Finkel and Holbrook, 2000). It has been implicated in many neurological diseases, such as stroke (van Leyen et al., 2006), periventricular leukomalacia (Inder et al., 2002), Parkinson's disease (Thompson et al., 2000), and Alzheimer's disease (Behl et al., 1992, Behl et al., 1994). In this study, we investigated the cellular signaling events following AA-induced oxidative death in OLs,

astrocytes, and neurons. We demonstrate that following AA treatment, OLs, astrocytes, and neurons undergo oxidative injury-induced cell death through different mechanisms.

In OLs, AA induces oxidative stress-mediated necroptotic cell death, as indicated by the protective effect of both 12- LOX and RIP-1 inhibitors (Figure 5, 11). This is in agreement with previous findings (Kim et al., 2010) showing that AA treatment leads to receptor-independent RIP-1 activation. Astrocytes were protected by 12-LOX and RIP-1 inhibitors from AA-induced oxidative stress as well. However, they undergo different morphological changes, namely a noticeable increase in lysosome formation. This was observed both through live cell imaging and pharmacological inhibition (Figure 7, 8). Treatment of astrocytes with autophagosome inhibitors was only mildly protective, but not statistically significant (Figure 8). Oxidative stress can be exacerbated by other cellular events, such as heavy metal release. Zinc has been implicated in oxidative stress (Zhang et al., 2007). Increases in intracellular levels have been shown to lead to rapid cell death (Choi and Koh, 1998, Frederickson et al., 2005). Zinc has also been shown to be associated with autophagic vacuoles (Lee et al., 2009). We found that astrocytes, OLs, and neurons were all protected by zinc chelation (Figure 10). It is possible that oxidative stress caused by AA metabolism leads to zinc release, which in turn causes lysosome formation and RIP-1, 12-LOX, and JNK activation. Further research is needed to elucidate the mechanism that leads to zinc release and whether zinc release is an upstream event in AA-induced oxidative cell death in astrocytes, OLs, and neurons.

Neurons, we observed, undergo oxidative stress when treated with AA. The mechanisms that lead to their cell death, however, differ markedly from that of OLs and

astrocytes. Neither 12-LOX nor JNK inhibition had any protective effect in neurons (Figure 6). Only vitamin K_2 and α-tocopherol were partially protective (Figure 6). Necrostatin-1 was also ineffective (Figure 11), in agreement with very low expression of RIP-1 and RIP-3 proteins in neurons (Figure 12). The positive RIP-1 mRNA expression we found via PCR could be due to astrocyte contamination (approximately 5%), as we were able to amplify GFAP from RNA samples isolated from mature neuron cultures (Figure 12A). At the protein level, however, RIP-1 is undetectable and would therefore be non-functional in neurons (Figure 12B, C). Considerable further research is needed to elucidate the mechanisms underlying AA-induced neuronal oxidative death.

It is very intriguing that neurons do not express significant amounts of RIP-1. In animal models of cerebral hypoxia/ischemia (Degterev et al., 2005), The RIP-1 inhibitor, necrostatin-1, has been shown to reduce infarct volume, suggesting that necroptosis is an important event in cerebral hypoxia/ischemia. However, the cellular target of necrostatin-1 has yet to be established. Our results suggest that the protection may actually be due nectrostatin-1's effect on glial cells (Allen and Barres, 2005, Freeman and Doherty, 2006, Wang and Bordey, 2008, Allen and Barres, 2009).

In conclusion, our study suggests that CNS cells possess different cell death mechanisms and responses to oxidative stress as well as shared mediators such as ROS and zinc (Figure 14). This could be of importance in conditions in which increases in AA levels and oxidative stress are important pathological events. Based on our findings, glial cells appear to have similar cell death mechanisms that are distinct from the neuronal population, influencing potential therapeutic strategies. This expands upon

previous research showing an *in-vivo* protective effect of necrostatin-1 in animal models of stroke (Degterev et al., 2005). Taken together, our results imply that protected glial cells possess the ability to maintain neuronal health in a harsh environment. Future research will be needed to deduce how glial cells provide this support under these conditions.

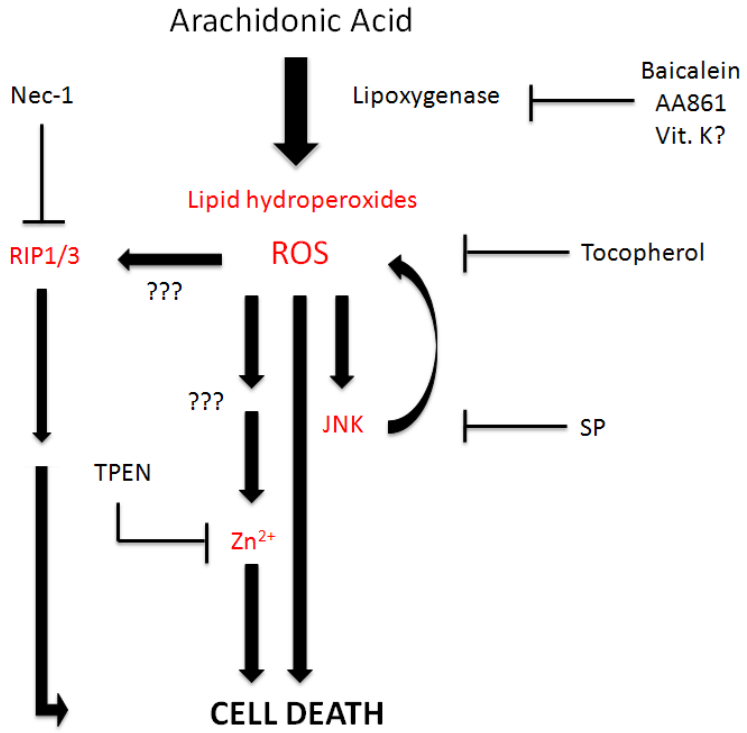

Figure 14 – Proposed schematic of arachidonic acid-induced toxicity. AA is metabolized primarily by lipoxygenases, which leads to lipid hydroperoxide and ROS production. This can be inhibited with baicalein, AA861, or vitamin K_2. ROS can be eliminated by tocopherol. ROS production leads to activation of RIP-1/3 and JNK. RIP-1 can be blocked by necrostatin-1 and JNK can be blocked by SP600125. ROS production also leads to zinc release, which can be attenuated by the zinc chelator TPEN.

REFERENCES

Allen NJ, Barres BA (2005) Signaling between glia and neurons: focus on synaptic plasticity. Curr Opin Neurobiol 15:542-548.

Allen NJ, Barres BA (2009) Glia - more than just brain glue. Nature 457:675-677.

Barres B, Hart I, Coles H, Burne J, Voyvodic J, Richardson W, Raff M (1992) Cell Death and Control of Cell Survival in the Oligodendrocyte Lineage. Cell 70:31-46.

Barres B, Raff M (1994) Control of Oligodendrocyte Number in the Developing Rat Optic Nerve. Neuron 12:935-942.

Barres B, Raff M (1999) Axonal Control of Oligodendrocyte Development. J Cell Biol 147:1123-1128.

Baumann N, Pham-Dinh D (2001) Biology of Oligodendrocyte and Myelin. Physiol Rev 81:871-927.

Behl C, Davis J, Cole GM, Schubert D (1992) Vitamin E protects nerve cells from amyloid βprotein toxicity. Biochem Biophys Res Comm 186:944-950.

Behl C, Davis JB, Lesley R, Schubert D (1994) Hydrogen peroxide mediates amyloid β protein toxicity. Cell 77:817-827.

Bunge R (1968) Glial Cells and the Central Myelin Sheath. Physiol Rev 48:197-251.

Burguillos MA, Deierborg T, Kavanagh E, Persson A, Hajji N, Garcia-Quintanilla A, Cano J, Brundin P, Englund E, Venero JL, Joseph B (2011) Caspase signalling controls microglia activation and neurotoxicity. Nature 472:319-324.

Busso D, Dominguez C, Perez-Acle T, Moreno RD (2010) Life-giving caspases: revealing new roles during mouse embryo preimplantation development. Int J Dev Biol 54:857-865.

Chavez-Valdez R, Martin LJ, Flock DL, Northington FJ (2012) Necrostatin-1 attenuates mitochondrial dysfunction in neurons and astrocytes following neonatal hypoxia–ischemia. Neurosci 219:192-203.

Choi DW, Koh JY (1998) Zinc and Brain Injury. Annu Rev of Neurosci 21:347-375.

Degterev A, Hitomi J, Germscheid M, Ch'en IL, Korkina O, Teng X, Abbott D, Cuny GD, Yuan C, Wagner G, Hedrick SM, Gerber SA, Lugovskoy A, Yuan J (2008) Identification of RIP1 kinase as a specific cellular target of necrostatins. Nat Chem Biol 4:313-321.

Degterev A, Huang Z, Boyce M, Li Y, Jagtap P, Mizushima N, Cuny GD, Mitchison TJ, Moskowitz MA, Yuan J (2005) Chemical inhibitor of nonapoptotic cell death with therapeutic potential for ischemic brain injury. Nat Chem Biol 1:112-119.

Duprez L, Takahashi N, Van Hauwermeiren F, Vandendriessche B, Goossens V, Vanden Berghe T, Declercq W, Libert C, Cauwels A, Vandenabeele P (2011) RIP Kinase-Dependent Necrosis Drives Lethal Systemic Inflammatory Response Syndrome. Immunity 35:908-918.

Feng Y, Fratkin JD, LeBlanc MH (2003) Inhibiting caspase-8 after injury reduces hypoxic-ischemic brain injury in the newborn rat. Eur J of Pharmacol 481:169-173.

Finkel T, Holbrook NJ (2000) Oxidants, oxidative stress and the biology of ageing. Nature 408:239-247.

Frederickson CJ, Koh J-Y, Bush AI (2005) The neurobiology of zinc in health and disease. Nat Rev Neurosci 6:449-462.

Freeman MR, Doherty J (2006) Glial cell biology in Drosophila and vertebrates. Trends Neurosci 29:82-90.

Friedlander R, Brown R, Gagliardini V, Wang J, Yuan J (1997) Inhibition of ICE slows ALS in mice. Nature 338:31.

Galvan V, Gorostiza OF, Banwait S, Ataie M, Logvinova AV, Sitaraman S, Carlson E, Sagi SA, Chevallier N, Jin K, Greenberg DA, Bredesen DE (2006) Reversal of Alzheimer's-like pathology and behavior in human APP transgenic mice by mutation of Asp664. Proc Natl Acad Sci U S A 103:7130-7135.

Gourine AV, Kasymov V, Marina N, Tang F, Figueiredo MF, Lane S, Teschemacher AG, Spyer KM, Deisseroth K, Kasparov S (2010) Astrocytes Control Breathing Through pH-Dependent Release of ATP. Science 329:571-575.

Gregory CD, Pound JD (2011) Cell death in the neighbourhood: direct microenvironmental effects of apoptosis in normal and neoplastic tissues. J Pathol 223:178-195.

Hardy R, Reynolds R (1991) Proliferation and differentiation potential of rat forebrain oligodendroglial progenitors both *in vitro* and *in vivo*. Dev 111:1061-1080.

Hidalgo A, ffrench-Constant C (2003) The control of cell number during central nervous system development in flies and mice. Mech Dev 120:1311-1325.

Hu BR, Liu CL, Ouyang Y, Blomgren K, Siesjo BK (2000) Involvement of Caspase-3 in Cell Death After Hypoxia-Ischemia Declines During Brain Maturation. J Cereb Blood Flow and Metab 20:1294-1300.

Inder T, Mocatta T, Darlow B, Spencer C, Volpe JJ, Winterbourn C (2002) Elevated Free Radical Products in the Cerebrospinal Fluid of VLBW Infants with Cerebral White Matter Injury. Pediatr Res 52:213-218.

Jacobson MD, Weil M, Raff MC (1997) Programmed Cell Death in Animal Development. Cell 88:347-354.

Katsuki H, Okuda S (1995) Arachidonic acid as a neurotoxic and neurotrophic substance. Prog Neurobiol 46:607-636.

Kerr JF, Wyllie AH, Currie AR (1972) Apoptosis: A Basic Biological Phenomenon with Wideranging Implications in Tissue Kinetics. Br J Cancer 26:239-257.

Kim S, Dayani L, Rosenberg PA, Li J (2010) RIP1 kinase mediates arachidonic acid-induced oxidative death of oligodendrocyt precursors. Int J Physiol Pathophysiol Pharmacol 2:137-147.

Koenig A, Russell JQ, Rodgers WA, Budd RC (2008) Spatial differences in active caspase-8 defines its role in T-cell activation versus cell death. Cell Death and Differentiation 15:1701-1711.

Kuo J, Lo C, Chang C, Lin H, Lin M, Chio C (2010) Brain cooling-stimulated angiogenesis and neurogenesis attenuated traumatic brain injury in rats. J Trauma 69:1467-1472.

Lee SJ, Cho KS, Koh JY (2009) Oxidative injury triggers autophagy in astrocytes: the role of endogenous zinc. Glia 57:1351-1361.

Lesuisse C, Martin LJ (2002) Immature and Mature Cortical Neurons Engage Different Apoptotic Mechanisms Involving Caspase-3 and the Mitogen-Activated Protien Kinase Pathway. J Cereb Blood Flow and Metab 22:935-950.

Levison S, Goldman J (1993) Both Oligodendrocytes and Astrocytes Develop from Progenitors in the Subventricular Zone of Postnatal Rat Forebrain. Neuron 10:201-212.

Li J, Wang H, Rosenberg PA (2009) Vitamin K prevents oxidative cell death by inhibiting activation of 12-lipoxygenase in developing oligodendrocytes. J Neursci Res 87:1997-2005.

Liang SL, Carlson GC, Coulter DA (2006) Dynamic regulation of synaptic GABA release by the glutamate-glutamine cycle in hippocampal area CA1. J Neurosci 26:8537-8548.

Linkermann A, Brasen JH, Himmerkus N, Liu S, Huber TB, Kunzendorf U, Krautwald S (2012) Rip1 (receptor-interacting protein kinase 1) mediates necroptosis and contributes to renal ischemia/reperfusion injury. Kidney Int 81:751-761.

McCarthy K, de Vellis J (1980) Preparation of Separate Astroglial and Oligodendroglial Cell Cultures from Rat Cerebral Tissue. J Cell Biol 85:890-902.

Metzstein M, Stanfield G, Horvitz H (1998) Genetics of programmed cell death in C. elegans: past, present, and future. Trends Genet 14:410-416.

Moos T, Rosengren Nielsen T, Skjorringe T, Morgan EH (2007) Iron trafficking inside the brain. J Neurochem 103:1730-1740.

Nakamura T, Lipton SA (2009) Cell death: protein misfolding and neurodegenerative diseases. Apoptosis 14:455-468.

Nave KA (2010) Myelination and support of axonal integrity by glia. Nature 468:244-252.

Nedergaard M, Ransom B, Goldman SA (2003) New roles for astrocytes: Redefining the functional architecture of the brain. Trends Neurosci 26:523-530.

Nicolay DJ, Doucette JR, Nazarali AJ (2007) Transcriptional control of oligodendrogenesis. Glia 55:1287-1299.

Oerlemans MI, Liu J, Arslan F, den Ouden K, van Middelaar BJ, Doevendans PA, Sluijter JP (2012) Inhibition of RIP1-dependent necrosis prevents adverse cardiac remodeling after myocardial ischemia-reperfusion in vivo. Basic Res Cardiol 107:270.

Ona V, Li M, Vonsattel J, Andrews L, Khan S, Chung W, Frey A, Menon A, Li X, Stieg P, Yuan J, Penney J, Young A, Cha J, Friedlander R (1999) Inhibition of caspase-1 slows disease progression in a mouse model of Huntington's disease. Nature 339:263-267.

Phillis JW, Horrocks LA, Farooqui AA (2006) Cyclooxygenases, lipoxygenases, and epoxygenases in CNS: Their role and involvement in neurological disorders. Brain Res Rev 52:201-243.

Pringle N, Mudhar H, Collarini E, Richardson W (1992) PDGF receptors in the rat CNS: during last neurogenesis, PDGF alpha-receptor expression appears to be restricted to glial cells of the oligodendrocyte lineage. Development 115:535-551.

Qin J, Berdyshev E, Goya J, Natarajan V, Dawson G (2010) Neurons and oligodendrocytes recycle sphingosine 1-phosphate to ceramide: significance for apoptosis and multiple sclerosis. J Biol Chem 285:14134-14143.

Raff MC (1998) Cell suicide for beginners. Nature 396:119-122.

Sakamaki K, Inoue T, Asano M, Sudo K, Kazama H, Sakagami J, Sakata S, Ozaki M, Nakamura S, Toyokuni S, Osumi N, Iwakura Y, Yonehara S (2002) Ex-vivo whole-embryo culture of caspase-8 deficient embryos normalize their aberrant phenotypes in the developing neural tube and heart. Cell death and differentiation 9.

Siegel RM (2006) Caspases at the crossroads of immune-cell life and death. Nat Rev Immunol 6:308-317.

Simonian NA, Coyle JT (1996) Oxidative Stress in Neurodegenerative Diseases. Annu Rev Pharmacol Toxicol 36:83-106.

Thompson CM, Capdevila JH, Strobel HW (2000) Recombinant Cytochrome P450 2D18 Metabolism of Dopamine and Arachidonic Acid. J Pharmacol Exp Ther 294:1120-1130.

Tiffany-Castiglioni E, Hong S, Qian Y (2011) Copper handling by astrocytes: Insights into neurodegenerative diseases. Int J Dev Neurosci 29:811-818.

Vallstedt A, Klos JM, Ericson J (2005) Multiple dorsoventral origins of oligodendrocyte generation in the spinal cord and hindbrain. Neuron 45:55-67.

van Leyen K, Kim HY, Lee SR, Jin G, Arai K, Lo EH (2006) Baicalein and 12/15-lipoxygenase in the ischemic brain. Stroke 37:3014-3018.

Vandenabeele P, Declercq W, Van Herreweghe F, Vanden Berghe T (2010) The Role of the Kinases RIP1 and RIP3 in TNF-Induced Necrosis. Sci Signal 3:1-8.

Varfolomeev EE, Schuchmann M, Luria V, Chiannilkulchai N, Beckmann JS, Mett IL, Rebrikov D, Brodianski VM, Kemper OC, Kollet O, Lapidot T, Soffer D, Sobe T, Avraham KB, Goncharov T, Holtmann H, Lonai P, Wallach D (1998) Targeted Disruption of the Mouse Caspase 8 Gene Ablates Cell Death Induction by the TNF Receptors, Fas/Apo1, and DR3 and Is Lethal Prenatally. Immunity 9:267-276.

Wang DD, Bordey A (2008) The astrocyte odyssey. Prog Neurobiol 86:342-367.

Weiss JH, Sensi SL, Koh JY (2000) Zn2+: a novel ionic mediator of neural injury in brain disease. Trends in Pharmacol Sci 21:395-401.

Xin M, Yue T, Ma Z, Wu FF, Gow A, Lu QR (2005) Myelinogenesis and axonal recognition by oligodendrocytes in brain are uncoupled in Olig1-null mice. J Neurosci 25:1354-1365.

Yang F, Sun X, Beech W, Teter B, Wu S, Sigel J, Vinters H, Frautschy S, Cole G (1998) Antibody to Caspase-Cleaved Actin Detects Apoptosis in Differentiated Neuroblastoma and Plaque-Associated Neurons and Microglia in Alzheimer's Disease. A J Pathol 152:379-389.

You Z, Savitz SI, Yang J, Degterev A, Yuan J, Cuny GD, Moskowitz MA, Whalen MJ (2008) Necrostatin-1 reduces histopathology and improves functional outcome after controlled cortical impact in mice. J Cereb Blood Flow Metab 28:1564-1573.

Yuan J, Shaham S, Ledoux S, Ellis HM, Horvitz HR (1993) The C. elegans cell death gene ced-3 encodes a protein similar to mammalian interleukin-1β-converting enzyme. Cell 75:641-652.

Yuan J, Yankner BA (2000) Apoptosis in the nervous system. Nature 407:802-809.

Zhang Y, Aizenman E, DeFranco DB, Rosenberg PA (2007) Intracellular zinc release, 12-lipoxygenase activation and MAPK dependent neuronal and oligodendroglial death. Mol Med 13:350-355.

Zhao Y, Sui X, Ren H (2010) From procaspase-8 to caspase-8: revisiting structural functions of caspase-8. J Cell Physiol 225:316-320.